Exploring Mechanisms to Resolve Position and Intensity Disparities to Create a Combined Sidescan and Multibeam Sonar Backscatter Image

By:

Clinton Marcus

UNH CEPS/CCOM

M.S. Directed Research Report

Directed Research Project Advisors:

Andrew A. Armstrong, Capt. NOAA (retired)
Co-Director, NOAA/UNH Joint Hydrographic Center
Affiliate Professor, University of New Hampshire

Dr. John Hughes Clarke
Professor, University of New Hampshire

THE UNIVERSITY OF NEW HAMPSHIRE
December 21, 2021

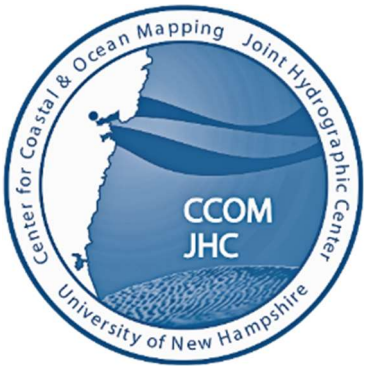

Contents

Table of Figures iii
Abstract 1
Introduction 1
The Need for Better Characterization 1
Full Coverage of the Seafloor 3
Sidescan Sonar 6
Multibeam Echosounder Bathymetry and Backscatter 10
Multibeam Acoustic Backscatter 13
Methods 16
Experiment Design 16
Location 17
Data Acquisition 20
R/V *Gulf Surveyor* 20
Sidescan Sonar System 21
Multibeam Echosounder System 24
System Calibrations 26
Data Acquisition 29
Data Processing 30
Sidescan Sonar 30
Multibeam Echosounder 34
Multibeam Acoustic Backscatter 37
Data Analysis 39
SSS and MBES Positioning Correlation and Analysis 39
SSS and MBES Backscatter Intensity Analysis 42
Discussion 49
Acknowledgements: 51
References: 52

Table of Figures

Figure 1: Portrayal of a single MBES swath. 2
Figure 2: Portrayal of multiple MBES swath coverage..... 3
Figure 3: Portrayal of a single SSS swath (towed), with the nadir zone highlighted in dark gray. 3
Figure 4: Portrayal of 100% SSS swath (bottom) with concurrent MBES (top) covering approximately 40% of the SSS. 3
Figure 5: On the top left is SSS data and on the top right, is the concurrently collected MBES backscatter data. The bottom image shows the two data sets with the MBES overlaid on the SSS. Example shows the need for a cohesive data product as the MBES data is insufficient, in and of itself, to provide accurate, full coverage characterization of the seafloor (NOAA Survey H13171). 5
Figure 6: Typical configuration of a towed SSS system. The broad across track and narrow along track beam is also seen (Capus et al. 2008). 7
Figure 6: SSS data showing the raw data on the left and the slant range corrected data on the right. The width of the water column is approximately 2 x the altitude. 8
Figure 8: From Crawford (2002) Effect of catenary and across track currents on towfish position. 9
Figure 9: Example of a typical Mills Cross sonar configuration (Degel et al. 2014)..... 11
Figure 10: Portrayal of transmit and receive pulses being narrow in the along-track dimension and wide in the across-track dimension (Diaz 1999)..... 12
Figure 11: Representation of an individual snippet with backscatter intensity at differing beam angles (Hughes Clarke 2020). 14
Figure 12: Bathymetry (top) with 5x vertical exaggeration compared to corresponding MBES backscatter (bottom). The diagram on the right shows the effect of grazing angle on the resulting backscatter strength. 15
Figure 13: Example of grazing angle and the effect of multibeam geometry and angular response curves of different sediment types (Hughes Clarke 2012)..... 16
Figure 14: Survey location showing previously collected full coverage MBES backscatter data from hydrographic survey W00501. 17
Figure 15: Overlay of seabed characteristics offshore of Odiornes Point. The black box is the NW survey area and the white box is the SE survey area. (https://maps.ccom.unh.edu/portal/apps/webappviewer/index.html?id=28df035fe82c423cb3517295d9bbc24c# Dec 10, 2021)..... 18
Figure 16: Image from the rocky portion of the NW survey area showing vegetation and the descriptive information for the site. (https://maps.ccom.unh.edu/portal/apps/webappviewer/index.html?id=28df035fe82c423cb3517295d9bbc24c#; Dec 10, 2021)..... 19
Figure 17: Image from the sand/mud portion of the NW survey area showing vegetation and the descriptive information for the site. (https://maps.ccom.unh.edu/portal/apps/webappviewer/index.html?id=28df035fe82c423cb3517295d9bbc24c#; Dec 10, 2021)..... 19
Figure 18: Image from the SE survey area depicting areas of gravel (dark green, right)) and gravel mixes (olive green, left).

(https://maps.ccom.unh.edu/portal/apps/webappviewer/index.html?id=28df035fe82c423cb3517295d9bbc24c#. Dec 10, 2021)..... 20
Figure 19: R/V Gulf Surveyor (http://ccom.unh.edu/facilities/research-vessels/rv-gulf-surveyor)..... 21
Figure 20: Diagram of RVGS with key locations and the offset of the towpoint to the reference point of the ship (not to scale). 21
Figure 21: Klein 4K-SVY Sidescan on deck of the R/V Gulf Surveyor with tow cable installed. 23
Figure 22: Example of typical SSS data with acoustic shadows, range scale, first return, and water column. 24
Figure 23: Kongsberg EM2040P MBES with Integrated Surface Sound Speed Probe. (https://www.kongsberg.com/maritime/products/ocean-science/mapping-systems/multibeam-echo-sounders/em-2040p-mkii-multibeam-echosounder-max.-550-m/)..... 25
Figure 24: EM2040P as installed on the center strut of the R/V Gulf Surveyor (Photo: Lt. Patrick Debroisse, NOAA). 26
Figure 25: Layout of SSS Lines for Position Confidence Checks at a 50m range scale..... 27
Figure 26: SSS contact positions (blue) in reference to the MBES target position (red). 28
Figure 27: Contact position errors in a geographic reference frame and in the Ship reference frame. Contact positions are predominately to the East of the MBES position. 28
Figure 28: SSS contact positions post application of Map Corrections. 29
Figure 29: SSS contact positions seen in a Geographic and Ship reference frame post-application of Map Corrections..... 29
Figure 30: Survey area with 60m and 80m line plans shown in red. 30
Figure 31: Cover Up mosaic (left) hiding contact vs. Shine Through mosaic (right) showing contact. 32
Figure 32: SSS mosaic showing all lines prior to having gain and positioning corrections applied, using Auto-All Data. Overlaid on RNC 13283. 33
Figure 33: SSS after having Map Corrections and EGN applied with the Auto-All Data visualization. 34
Figure 34: DTM (top) showing refraction artifacts and the same artifacts as seen in the ping data (bottom). 35
Figure 35: Full Coverage DTM of EM2040P MBES Data..... 36
Figure 36: DTM of EM2040P data after being filtered to 45º from nadir. 37
Figure 37: MBAB collected by EM2040P at 300 kHz with a 50cm resolution. The NW acquisition site is on the left and the SE acquisition site is on the right. Backscatter intensity is represented in decibels at the default scale of 10 to -70dB. 38
Figure 38: The NW MBES data after being adjusted to show a visual range of -4 to -28db..... 39
Figure 39: SSS contact position (left) and assumed "true" position from MBES (right). 40
Figure 40: Position of SSS contact after having the Map Correction applied. Original SSS position annotated with green marker..... 41
Figure 41: Another example of Pre (left) and Post (right) Map Corrections showing what initially appears to be two separate lines of lobster pots. 41
Figure 42: Disparity of ~7.5m between two SSS lines after having Map Corrections applied. The red box highlights the area where the sand waves should overlap. 42
Figure 43: NW acquisition site: MBES (top), SSS (middle), and MBES Backscatter (bottom) prior to being overlaid. 44
Figure 44: SE acquisition site: MBES (top), SSS (middle), and MBES Backscatter (bottom) prior to being overlaid. 45

Figure 45: Initial comparison of the NW MBES backscatter in dB with the SSS imagery. 46
Figure 46: NW SSS and MBAB data after being adjusted to match intensity visualization. 47
Figure 47: Initial comparison of the SE MBES backscatter in dB with the SSS imagery..... 48
Figure 48: SE SSS and MBAB data after being adjusted to match intensity visualization. 49

Abstract

The need for comprehensive seabed characterization has increased as fields such as offshore engineering and habitat management have expanded. Sidescan sonars and multibeam echosounders have traditionally been applied independently to provide high-resolution backscatter imagery of the seabed, as there are a number of factors such as different grazing angles and incompatible positioning uncertainty that have precluded a cohesive product using both sensors together. As part of this study, by using the "true" position of a feature from a multibeam grid to reposition sidescan navigation data, the associated sidescan imagery positions are now recalculated with a reduced uncertainty and agree with the multibeam bathymetry. Once all sidescan navigation has been recalculated, the more quantifiable multibeam backscatter strength estimates can be used to qualitatively adjust the level and dynamic range of the sidescan imagery to create a near homogenous backscatter mosaic of the seabed. By creating this combined product, one can now provide a full-coverage backscatter product with both greater positional accuracy and a relatively homogeneous visual scale. The combination of these mosaics from the two sources typically used by NOAA's Office of Coast Survey for bathymetric surveys, creates a new product that can be utilized by customers beyond those of Coast Survey's typical navigational charting communities.

Introduction

The Need for Better Characterization

Seafloor characterization has become one of the major areas of study for ocean scientists across an ever-growing array of fields. Commercial companies and governmental agencies alike rely on high-quality characterization of the seafloor for uses from fisheries habitat mapping to locating viable areas for offshore windfarms and other ocean engineering exploration (Barrie and Conway 2013; Lamarche and Lurton 2018; Shang et al. 2019).

In the United States, the release of the Presidential Memorandum on Ocean Mapping (84 FR 64699) highlights the need to find methods to obtain high-quality seabed imagery for the characterization of the U.S. Exclusive Economic Zone (EEZ) in a greater quantity and more efficiently.

A significant proportion of anthropogenic activity (e.g., navigation, wind energy, fisheries, oil, etc.) takes place in shallow coastal areas, which motivates the need for mapping and characterization in these regions (Hughes Clarke 2004). Most MBES systems can acquire swaths of depth measurements and backscatter imagery with seafloor coverage equal to four times water depth. In such shallow waters, the achievable coverage from multibeam echosounder (MBES) surveys is disproportionately ineffective when compared to sidescan sonars (SSS). In waters that are 10m or less in depth, this equates to a maximum of approximately 40m of useable swath width, whereas as SSS running a with 75m range scale can acquire 150m of coverage width in the same water depth. In the figures below, the difference between the swath coverage of SSS and MBES systems can be seen. Figure 4 shows how a MBES system can be used to cover the nadir zone, where the SSS imagery is ineffective. That zone, which is generally within +/-45 degrees of nadir, is where the sidescan has poor horizontal range resolution and often deliberately weak beam pattern sensitivity.

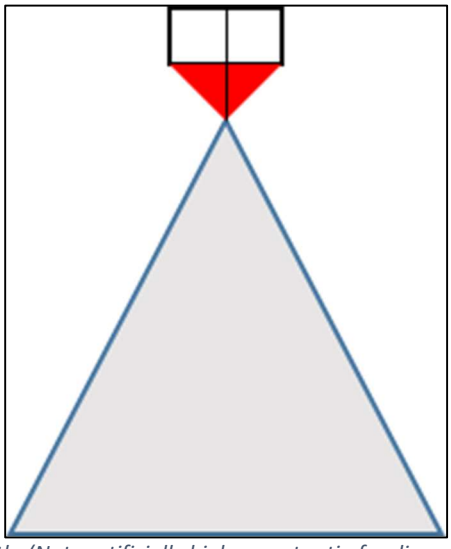

Figure 1: Portrayal of a single MBES swath. (Note artificially high aspect ratio for diagrammatic clarity, true swath is 4x altitude)

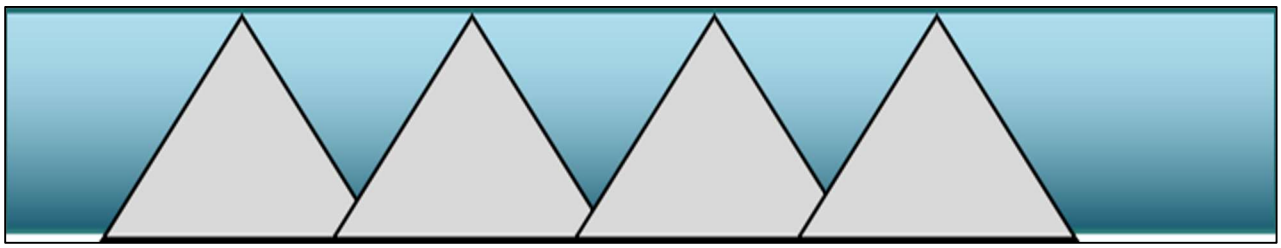

Figure 2: Portrayal of multiple MBES swath coverage.

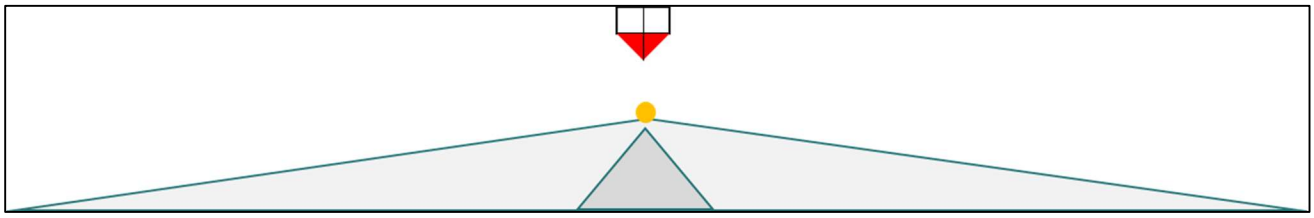

Figure 3: Portrayal of a single SSS swath (towed), with the nadir zone highlighted in dark gray.

Figure 4: Portrayal of 100% SSS swath (bottom) with concurrent MBES (top) covering approximately 40% of the SSS.

Given the large areas of relatively shallow water in the U.S. EEZ, the time and resources required to conduct a survey with 100% MBES coverage is difficult to justify (Fakiris et al. 2009; Hughes Clarke 2004). Due to these constraints, it has become commonplace, within the National Oceanic and Atmospheric Administration (NOAA), to use SSS with concurrent, but incomplete coverage, MBES to fully map these relatively shallow waters. The use of SSS allows shallow water surveys to be completed more efficiently, as line spacing is based on the range scale of the SSS, instead of being adjusted to provide for 100% MBES coverage.

Full Coverage of the Seafloor

NOAA hydrographic surveys are designed to provide complete coverage of the seafloor in line with international standards. NOAA considers SSS with 100% and 200% coverage with concurrent MBES to meet its requirements for *Complete Coverage* of the seafloor, and *Object Detection* of potential dangers to navigation, respectively, per the Office of Coast Survey Hydrographic Survey Specifications and Deliverables (HSSD) (HSSD 2021).

The HSSD defines the area ensonified by a single swath of SSS coverage as the “scanning coverage”. For hydrographic surveys, the scanning coverage of a given area is defined in terms of

percentage, with each 100% being cumulative. That is, if an area is ensonified once, it equates to 100% and each consecutive coverage equates to another 100%. For surveys that are to meet the *Complete Coverage* requirements of the HSSD, the seafloor is to be ensonified at least 100% by SSS coverage with the MBES data being collected concurrently with the same coverage requirement to cover the nadir region the SSS, at a minimum. When planning *Object Detection* surveys, the HSSD specifies that at least 200% of the seafloor is ensonified by SSS coverage with concurrent MBES that, at a minimum, covers the nadir gap of the SSS (HSSD 2021). Per the HSSD (2021), the second 100% of an *Object Detection* SSS survey can be collected in three different techniques:

1. "Conduct a single survey wherein the vessel track lines are separated by one-half the distance required for 100-percent coverage."
2. "Conduct two separate 100-percent coverages wherein the vessel track lines during the second coverage split the difference between the track lines of the first coverage. Final track spacing is essentially the same as technique 1."
3. "Conduct two separate 100-percent coverages in orthogonal directions. This technique may be advantageous when searching for small man-made objects on the bottom as the bottom is ensonified in different aspects. However, basic line spacing requirements for single-beam echo sounders may not be met when using this technique."

Each 100% of the SSS data is mosaicked separately, as is the MBES backscatter. Figure 5 below shows a typical example of an area with full scanning coverage of SSS (top left) with the concurrently collected MBES backscatter (top right). The bottom image is the combination of the two data sets with the MBES backscatter overlaid on the SSS imagery.

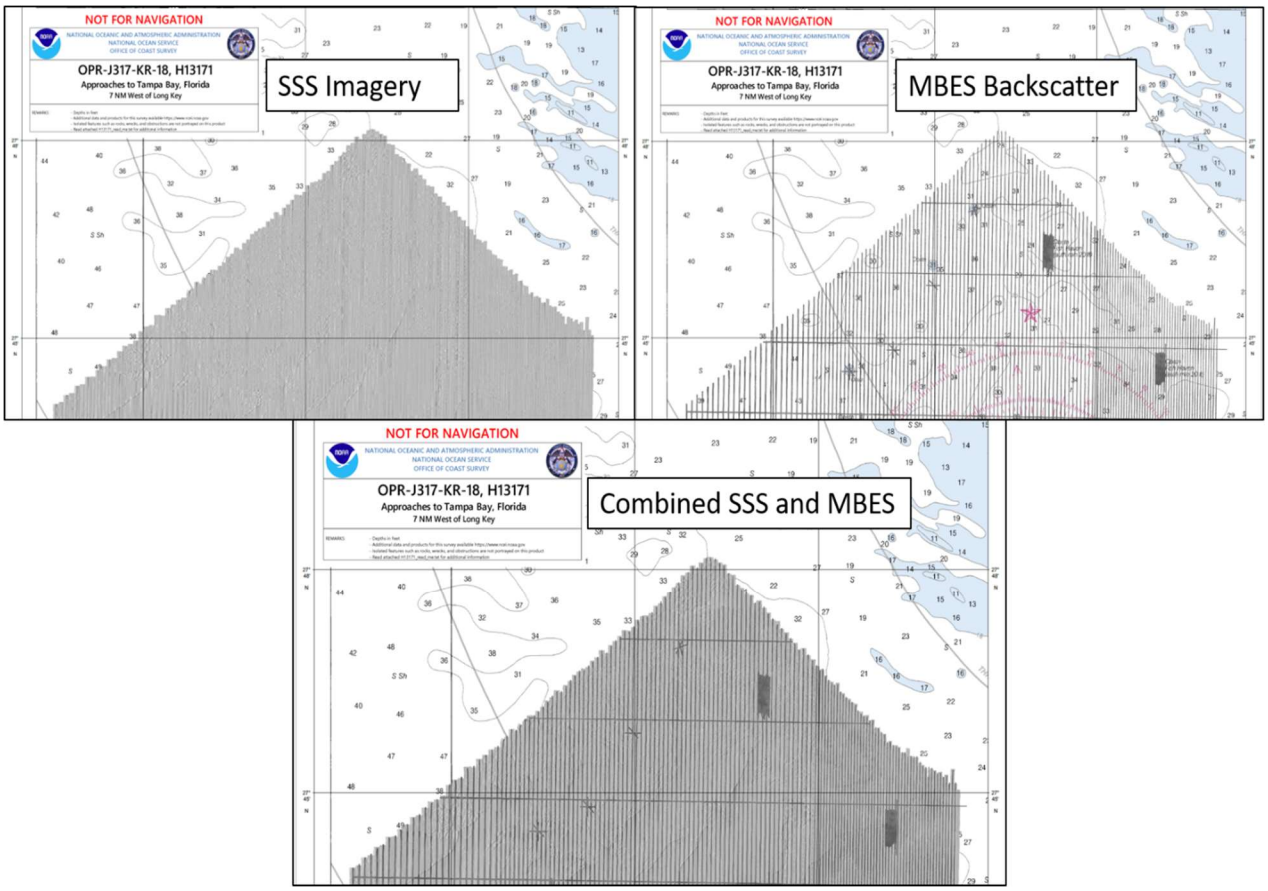

Figure 5: On the top left is SSS data and on the top right, is the concurrently collected MBES backscatter data. The bottom image shows the two data sets with the MBES overlaid on the SSS. Example shows the need for a cohesive data product as the MBES data is insufficient, in and of itself, to provide accurate, full coverage characterization of the seafloor (NOAA Survey H13171).

While the capabilities of SSS in shallow water are more effective than MBES in ensonifying the seafloor, several problems that exist that must be explored in order to be better suited for multiple seafloor characterization uses. Sidescan sonar systems provide excellent swath width and imagery in shallow water but are limited to acoustic time series imagery only with no true bathymetry and without accurate position registration on the seafloor or accurately quantified grazing angles. Conversely, MBES systems provide fine resolution imagery, commonly referred to as backscatter, or “pseudo-sidescan”, and co-registered bathymetry (Hughes Clarke 2012; Fakiris et al 2019), but are limited in swath width. Fakiris et al (2019) point out that while there has been previous work to compare the use of SSS and MBES, there is still a gap in the analysis of how these two systems might be used together to provide a more comprehensive and complementary characterization product in shallow water survey areas. The goal of this research is to explore mechanisms that currently exist in commercial software to create a

pathway for usefully combining SSS imagery with MBES backscatter that has been collected concurrently in a shallow-water survey.

Sidescan Sonar

Sidescan sonar systems are active sonars that transmit beams that are wide in the across-track dimension, and narrow in the along-track dimension. These arrays are typically mounted to a rigid body that can be either towed, affixed to the keel, or mounted on a pole that can be placed anywhere on a vessel (Capus et al. 2008). Sidescan sonars generally operate in a frequency range from 6 kHz to 1 MHz and these frequencies are usually dependent on the intended use (Capus et al. 2008; Blondel 2009). NOAA typically uses SSS systems in the range of 300 kHz to 900 kHz for their survey missions. The frequencies associated with SSS in this range present data that has a capability for high resolution imagery and the detection of small targets. It is not uncommon to get seafloor across- track resolutions of 1 cm with very high frequency SSS systems (Blondel 2009). In the ocean mapping community, SSS has historically been used for both seafloor characterization, and object detection. For NOAA charting surveys the main use of SSS is for detection of navigation hazards.

In figure 6 below, a typical towed configuration of a SSS and its beam form can be seen that illustrates the broad across track, and narrow along track beam widths (Capus et al. 2008). The nadir region is also seen in this image. This zone contains poor seafloor imagery, and its width is solely dependent on the altitude of the SSS and the bandwidth of the sonar. The poor quality is a result of two geometric factors: 1 - the sidescan only sampling in slant rage which, at high grazing angles, corresponds to poor horizontal range resolution and 2 – the sidescan usually having a weak or null beam pattern at those high grazing angles and thus having low source level and receiver sensitivity, resulting in a weak return. The closer to the seafloor the SSS is, the narrower the nadir “gap” (strictly zone of low quality ensonification). This factor is important when planning SSS with concurrent MBES surveys. One needs to ensure that the SSS nadir gap width does not exceed the maximum coverage swath of the MBES. The geometry of the nadir region is estimated during slant range correction, which uses a flat seafloor assumption, that takes the altitude and speed of sound to calculate the time of the first echo return

(Blondel 2009; Hughes Clarke 2004). The first returns from each channel are then stitched together by the software to remove the water column part of the sidescan trace from the mosaic. While slant range correction does provide echo estimates in the high grazing angle region, their quality is compromised due to the factors stated earlier. An example of SSS before and after slant range correction can be seen in figure 7 below.

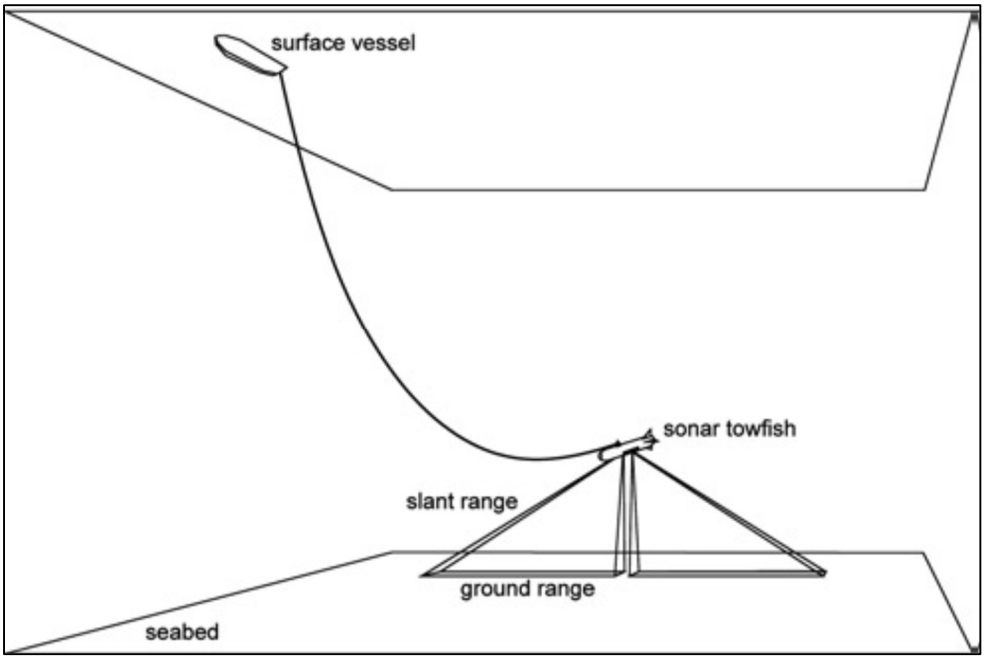

Figure 6: Typical configuration of a towed SSS system. The broad across track and narrow along track beam is also seen (Capus et al. 2008).

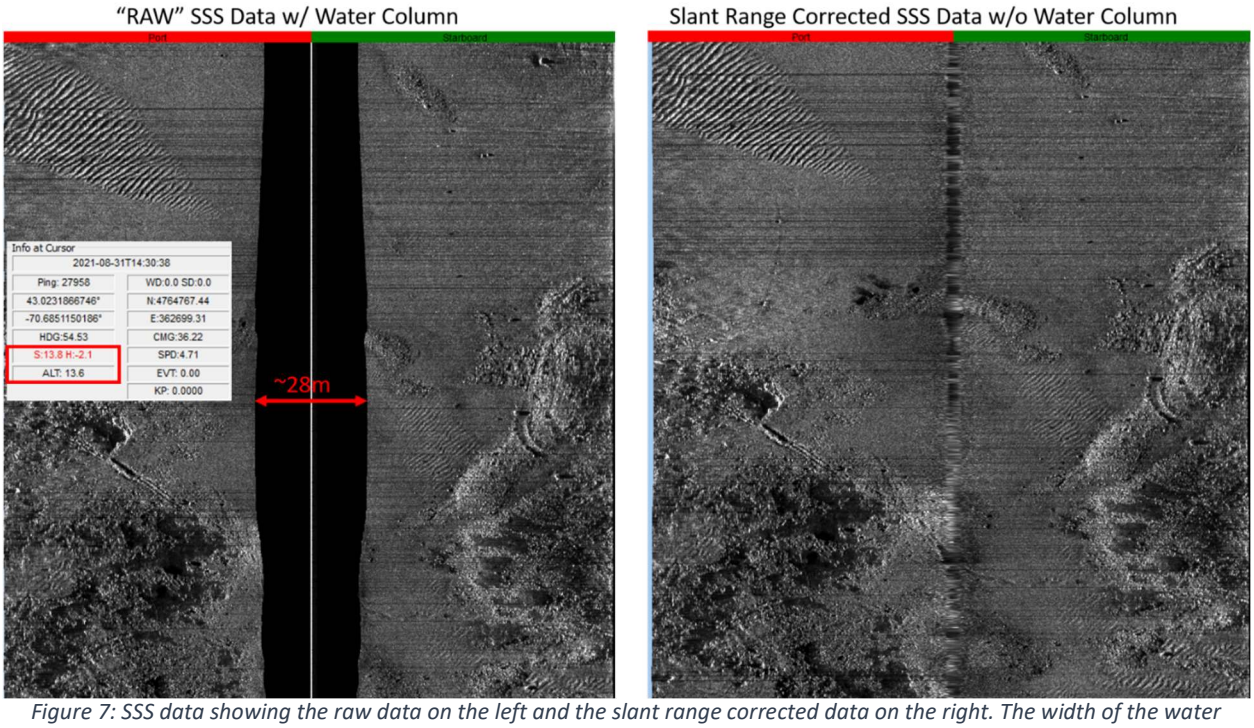

Figure 7: SSS data showing the raw data on the left and the slant range corrected data on the right. The width of the water column is approximately 2 x the altitude.

Due to the nature of its normally low grazing angles, the sonar beams reflect strongly off proud features or objects on the seabed and cast an acoustic shadow on the side of the feature that is not ensonified. This shadow can then be used to interpret the shape of the object and estimate the object's height and width. To get an accurate approximation of these measurements with a towed SSS, the height of the towfish above the seafloor has to be accurately known, and to establish a valid position of the object, the location and attitude of the towfish must be determined. For a towed system, this determination must consider the location of the towpoint relative to the positioning antenna, the amount of tow cable out, the catenary in the cable, the altitude of the sensor above the seafloor, the azimuth of the towbody and any other offsets in the position reference frame. This trigonometric relationship can help enhance the positioning uncertainty native to a towed system (Leblond, Bertholom 2020; Crawford 2002). In the image below, Crawford (2002) illustrates how a towed instrument can be affected by movement in both the vertical (top) and horizontal (bottom) axis. In the upper diagram, it can be seen how the towpoint offset, the amount of cable out, and the catenary in the cable affect the layback, which is the distance from the towfish to the ship. The lower diagram in the image shows how an across track current can affect the estimated position of the towfish in the horizontal dimension.

Even with accurate towfish location, imperfect heading sensors (typically magnetic compasses) can degrade a target location estimate as the target may be 75+m away.

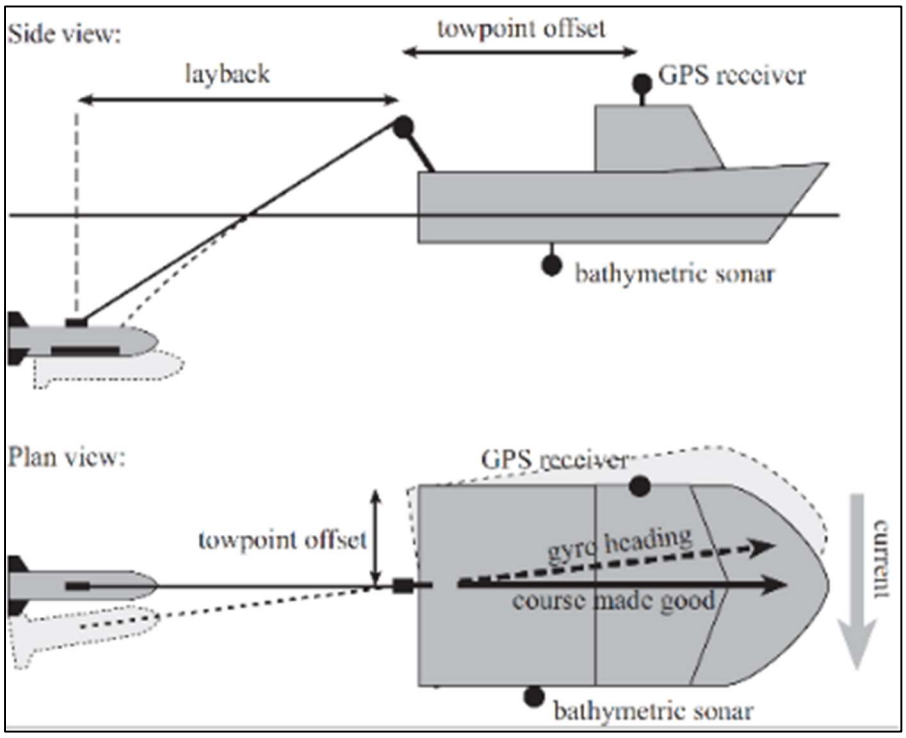

Figure 8: From Crawford (2002) Effect of catenary and across track currents on towfish position.

Multiple methods exist to enhance the positioning uncertainty native to towed systems. Acoustic positioning systems such as Short Baseline (SBL) use a transducer attached to a vessel, which receives a signal from the towfish (Fig. 9). These systems calculate the distance between the vessel and towfish by using the time delay between the transmission and receive pulses. The relative position of the towfish in these systems can be calculate with an accuracy of 1% for ranges up to 2,500m (Blondel 2009). Ultra Short Baseline (USBL) systems are similar and work by using the acoustic range and bearing of a vessel in conjuncture with the attitude information and GPS (Blondel 2009, Leblond and Bertholom 2020).

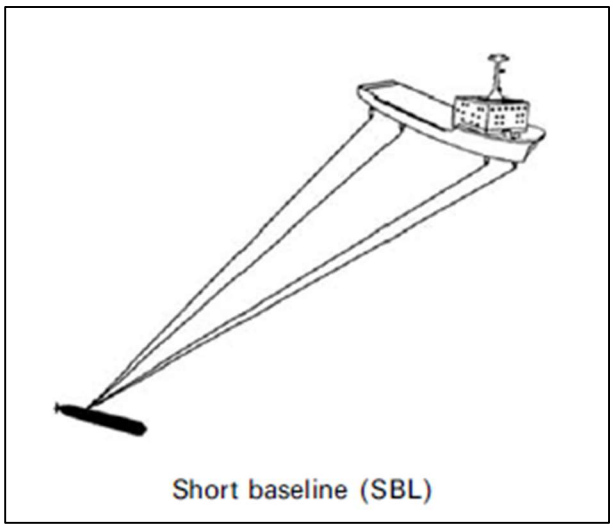

Figure 9: Example of an SBL system with transducers on the ship and towfish (Blondel 2009).

Another way to provide a more accurate positioning solution is to mount the SSS on a pole or on the keel of the vessel. While these methods reduce the positioning uncertainty, they are not without their own limitations (Hughes Clarke 2004). Fluctuations in attitude become much more pronounced when the SSS is fixed to the vessel, as opposed to being "decoupled" and independent of ship motion when in a towed configuration. In addition to the susceptibility to roll, pitch, and yaw, and the associated degradation of image quality and object detection, the data also loses the benefit of low grazing angles that are common with a towed system (Hughes Clarke 2004).

Multibeam Echosounder Bathymetry and Backscatter

As the need for more accurate charts and seabed characterization arose, sounding systems have evolved from simple lead-lines and wire drags, to single beam echosounders (SBES) in the 1920's, to SSS in the 1950's, and eventually the MBES systems that have become common place in the hydrographic mapping community today (Sternlicht 2017; Vilming 1998).

Transmit and receive arrays in most common multibeam systems are installed in a "Mills Cross" configuration forming a "T" shape (Fig. 10) (Degel et al. 2014). The transmit pulse is wide in the across-track dimension and narrow in the along-track dimension. The receive beams are formed in multiple across-track segments wide in the along-track dimension and narrow in the across-track dimension. The intersection of transmit and receive beams results in individual high-resolution beams across the swath

(Fig. 11) (Diaz 1999; Hellequin et al. 2003; Hughes Clarke 2012). Each pulse is computed to generate a sounding by measuring the two-way travel time and steering angle using estimations of amplitude or phase (Hellequin et al. 2003).

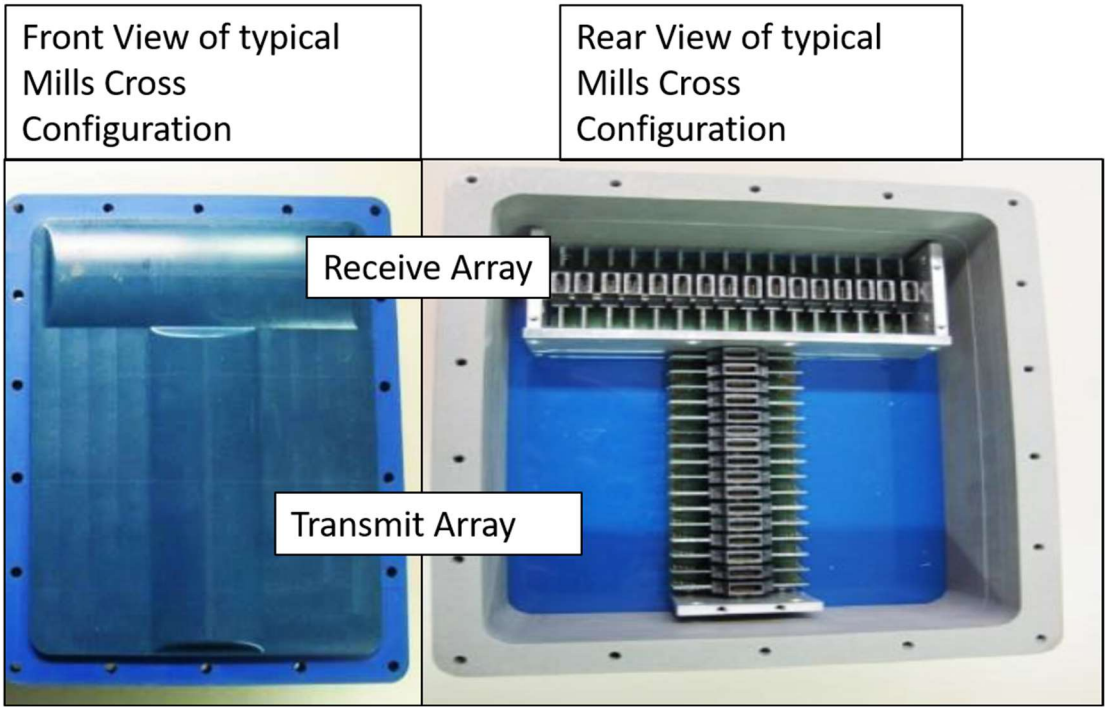

Figure 10: Example of a typical Mills Cross sonar configuration (Degel et al. 2014)

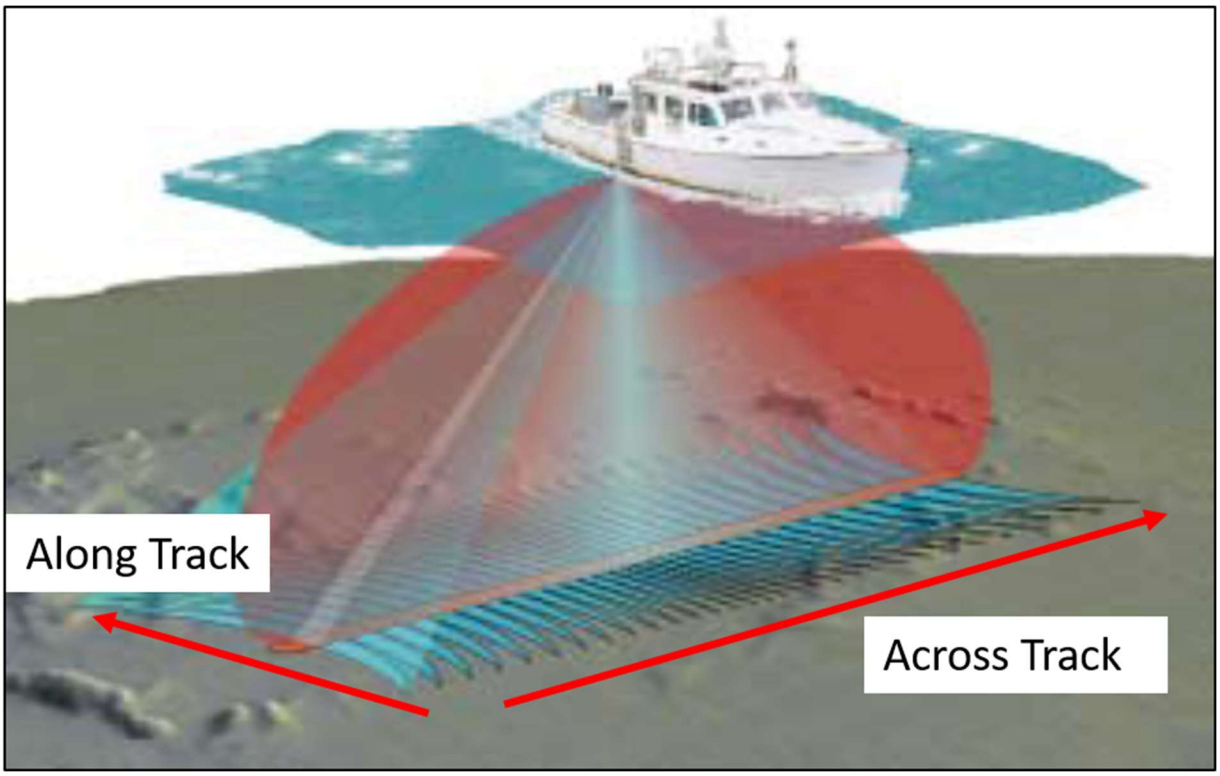

Figure 11: Portrayal of transmit and receive pulses being narrow in the along-track dimension and wide in the across-track dimension (Diaz 1999).

Modern MBES systems operate over a wide range of frequencies, and the systems are generally chosen depending on the depth at which they are needed to measure. "Low" frequency MBES (12 kHz – 30 kHz) are generally employed to map deep water ranging from > 400m down to over 10km. Multibeam sonars that use frequencies in the 100-300 kHz range are generally employed for water depths along the continental shelf, and MBES systems that are ≥ 400kHz are generally employed in waters < 75m. Higher frequency sonars suffer more attenuation due to absorption and are thus limited in depth range. Low frequency sonars are able to operate in most depths, but the resolution in shallow water suffers due to the typically lower bandwidth and the increase in size of the beam footprint given the same array length.

The beam footprints associated with MBES are directly related to both the along-track (transmit), and across-track (receive) beam widths, and the resolution available is limited by the size of the resulting footprint (Hughes Clarke 2012). With a given array length, the beam footprint increases in size as the frequency decreases and as the radius from the source increases. By increasing the number

of wavelengths along the array length, the beam width decreases which results in a smaller beam footprint.

Multibeam echosounders utilize high grazing angles, with the nadir incidence at 90º out to as low as 25º at the outer beams (Hughes Clarke 2012).The high grazing angles in MBES systems are excellent for bathymetry, as there are few acoustic shadows, and the return echo is relatively strong.

Multibeam Acoustic Backscatter

Along with bathymetric data, modern MBES systems also record the amplitude of the return as "snippets", which can provide information about the geomorphic structure of the seafloor (Hellequin et al. 2003). These snippets are extracted from each adjacent beam footprint time series. The ability to register data on topographically differing substrate is a result of the snippets being from a single receive channel and the limited range of elevation angles so that no layover of the footprints occurs (Hughes Clarke 2020). Snippet registration occurs through corresponding each line along the seabed through the geometric center of the transmit beam. The resulting mosaic is a result of stacking each adjacent beam in the across-track dimension. Unlike SSS, which assumes a flat seafloor, the MBES snippets are slant range corrected by estimating the across-track bathymetric profile (Hughes Clarke 2020).

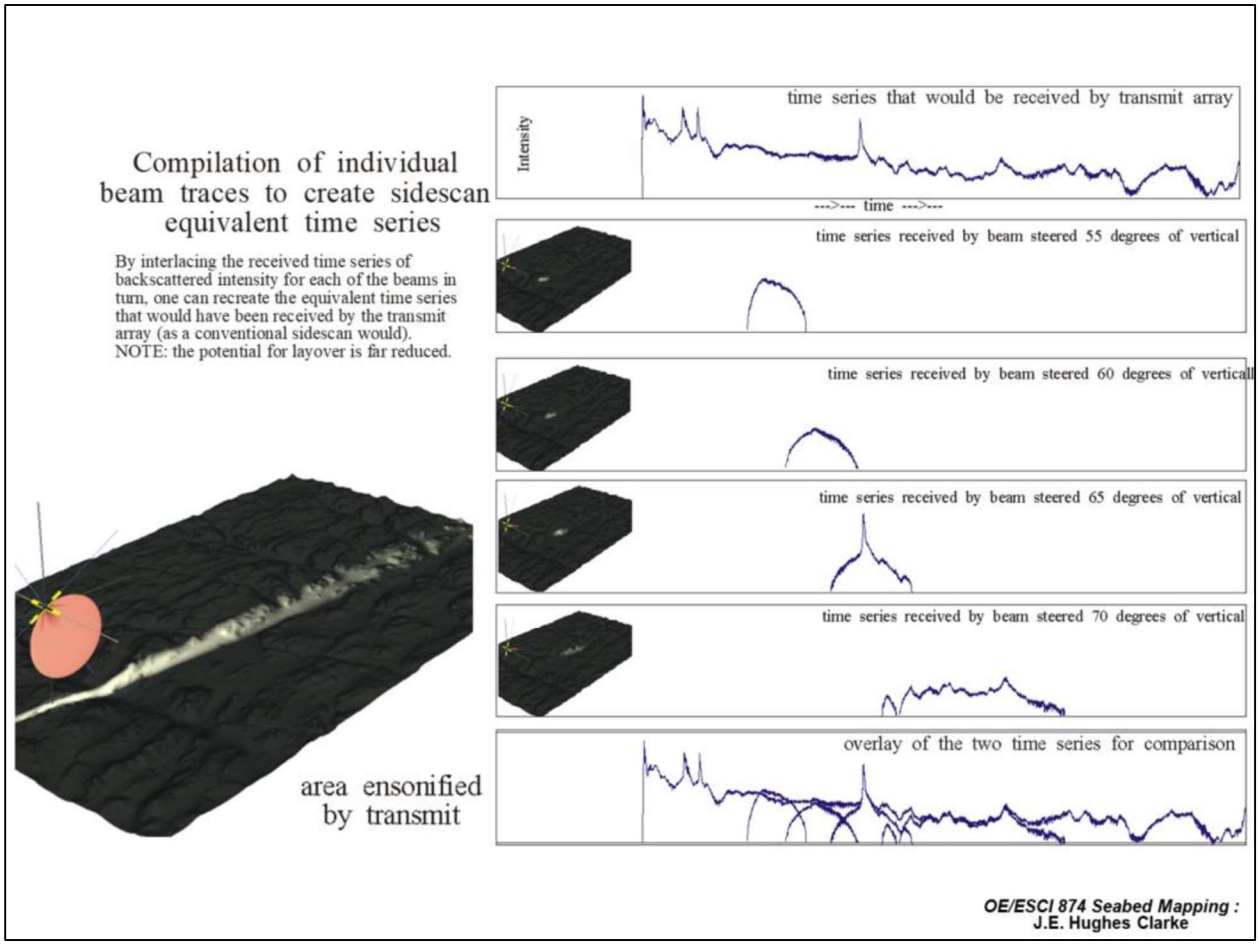

Figure 12: Representation of an individual snippet with backscatter intensity at differing beam angles (Hughes Clarke 2020).

The amplitude of the acoustic backscatter (BS) is commonly reduced to a measure of backscatter strength reported in decibels, and is generally shown as a gray scale image, with the shades of gray being proportional to the backscatter strength, and is precisely coregistered with the accompanying MBES bathymetry. The main difference between the bathymetry returned by an MBES and the backscatter is that backscatter shows the amplitude of the return indicative of the scattering properties of thes eabed, ideally independent of the depth measurement, whereas the bathymetry issolely the relief represented by the depth range (Fig. 13). The level of BS intensity returned is highly dependent on the grazing angle of the signal and the physical properties of the seafloor-water column interface (e.g., roughness and impedance) (Hughes Clarke 2012). Because of this strong grazing angle dependence there are limits on the interpretation of backscatter strength. Figure 14 from Hughes Clarke (2012) below shows how backscatter intensity is affected by grazing angle and the effect on the angular response.

The acoustic backscatter is extremely useful in providing information on the character of the seafloor due to the echo-strength of the return. Different seabed compositions reflect sound at different intensities, where “hard” substrates such as bedrock, boulders and gravel (high impedance contrast) return a higher BS level than “soft” substrates such as silt and mud (Fig. 14B). Figure 14B also illustrates how some sediments, such as sand, can show an increase in the backscatter strength when the grazing angle reaches near critical angle (Hughes Clarke 2012).

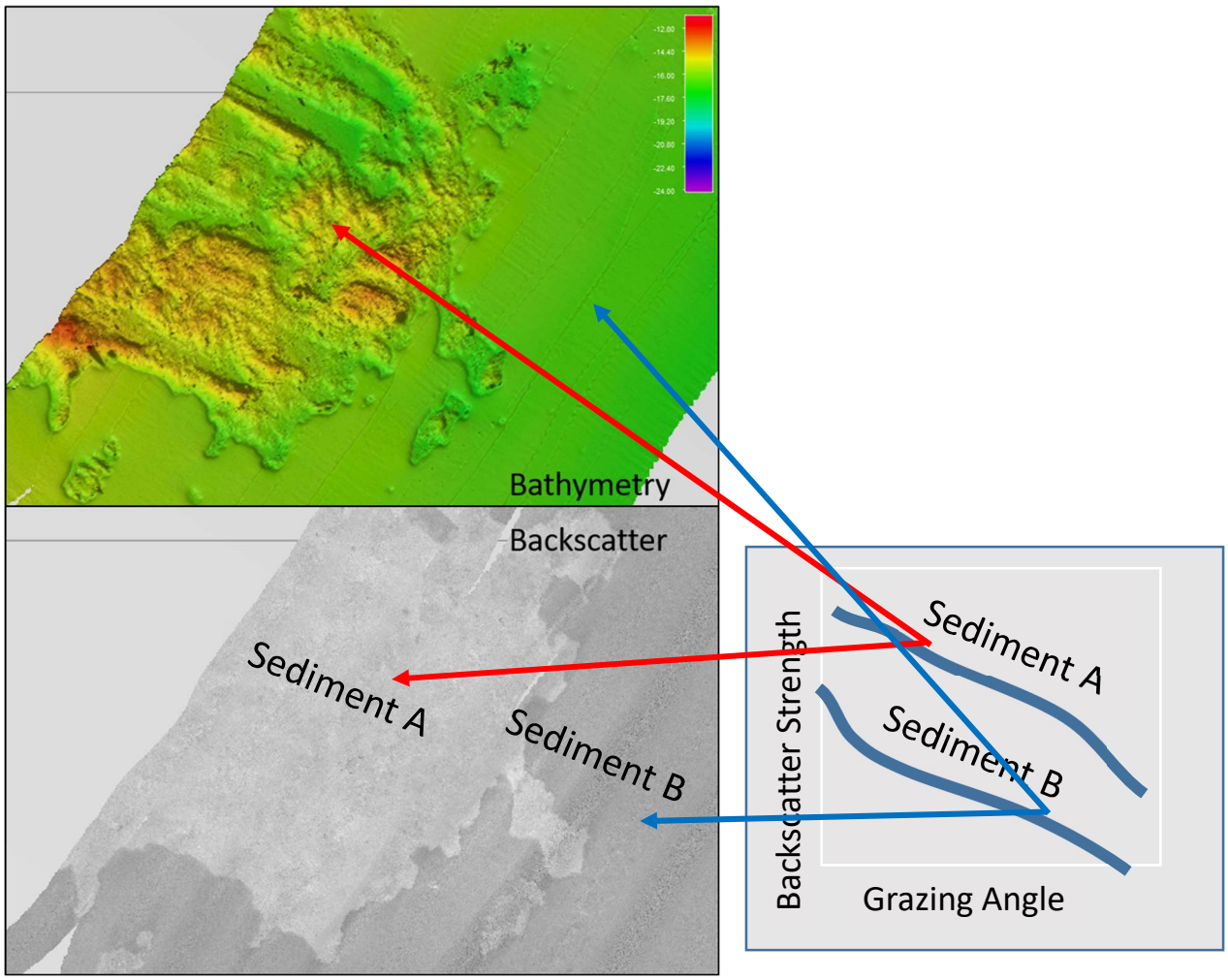

Figure 13: Bathymetry (top) with 5x vertical exaggeration compared to corresponding MBES backscatter (bottom). The diagram on the right shows the effect of grazing angle on the resulting backscatter strength.

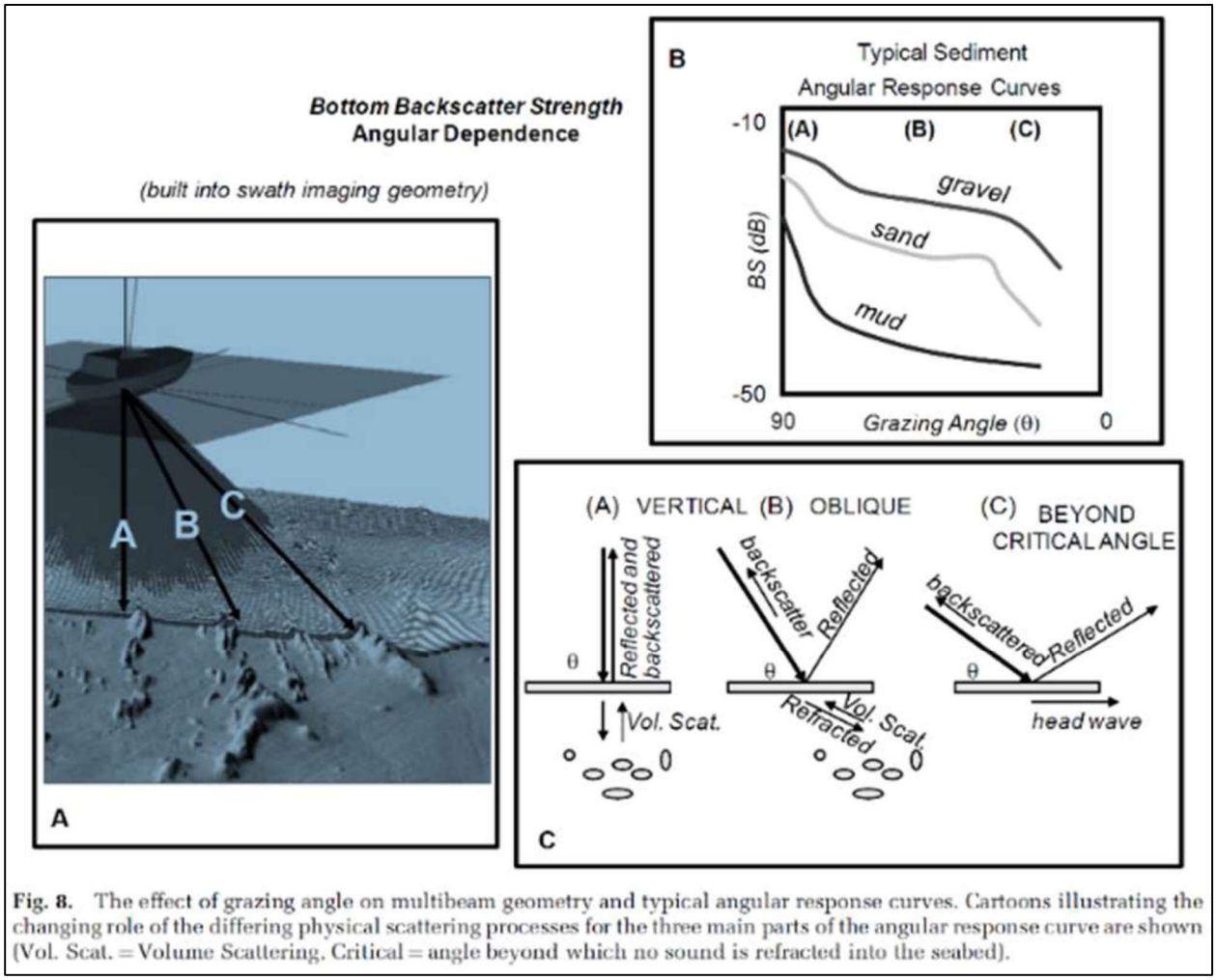

Fig. 8. The effect of grazing angle on multibeam geometry and typical angular response curves. Cartoons illustrating the changing role of the differing physical scattering processes for the three main parts of the angular response curve are shown (Vol. Scat. = Volume Scattering, Critical = angle beyond which no sound is refracted into the seabed).

Figure 14: Example of grazing angle and the effect of multibeam geometry and angular response curves of different sediment types (Hughes Clarke 2012)

Methods

Experiment Design

This experiment was designed to acquire and evaluate data that would meet the additional characterization benefit of dual system acquisition, specifically to investigate the capabilities of commercially available software to combine data from two different systems, SSS and MBES, for the purpose of integrated seabed classification and characterization. This project implements a controlled experiment where a test data set has been collected using a towed SSS configuration while concurrently acquiring MBES data. Both data sets were processed and analyzed to compare position and intensity for the purpose of creating a single cohesive product, specifically where MBES data does not provide full coverage.

Location

Data collection occurred in two different locations, approximately 1.6km and 3.1km, respectively, offshore from Odiornes Pt., New Hampshire. The known bottom characteristics from data acquired during previous surveys led to the informed decision to select these sites (Figs. 15 thru 19) (Hydrographic Survey 00501, Ward et al. 2021). The site closest to shore (NW) shows non-homogeneous characteristics, while the offshore site (SE) is relatively homogeneous in seafloor characteristics (Fig. 15). The two sites provide a strong basis for determining the capability of each sonar system, as well as the ability of the processing software to match the respective data sets qualitatively.

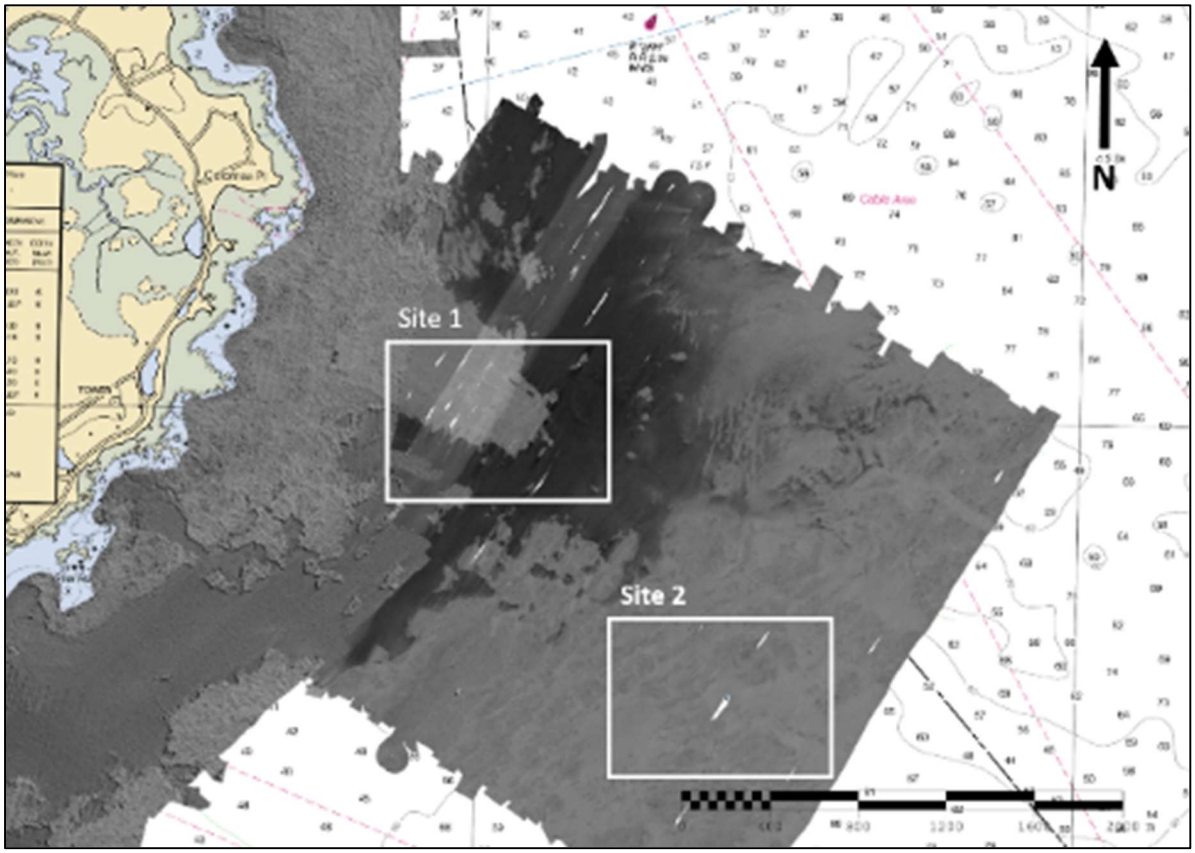

Figure 15: Survey location showing previously collected full coverage MBES backscatter data from hydrographic survey W00501.

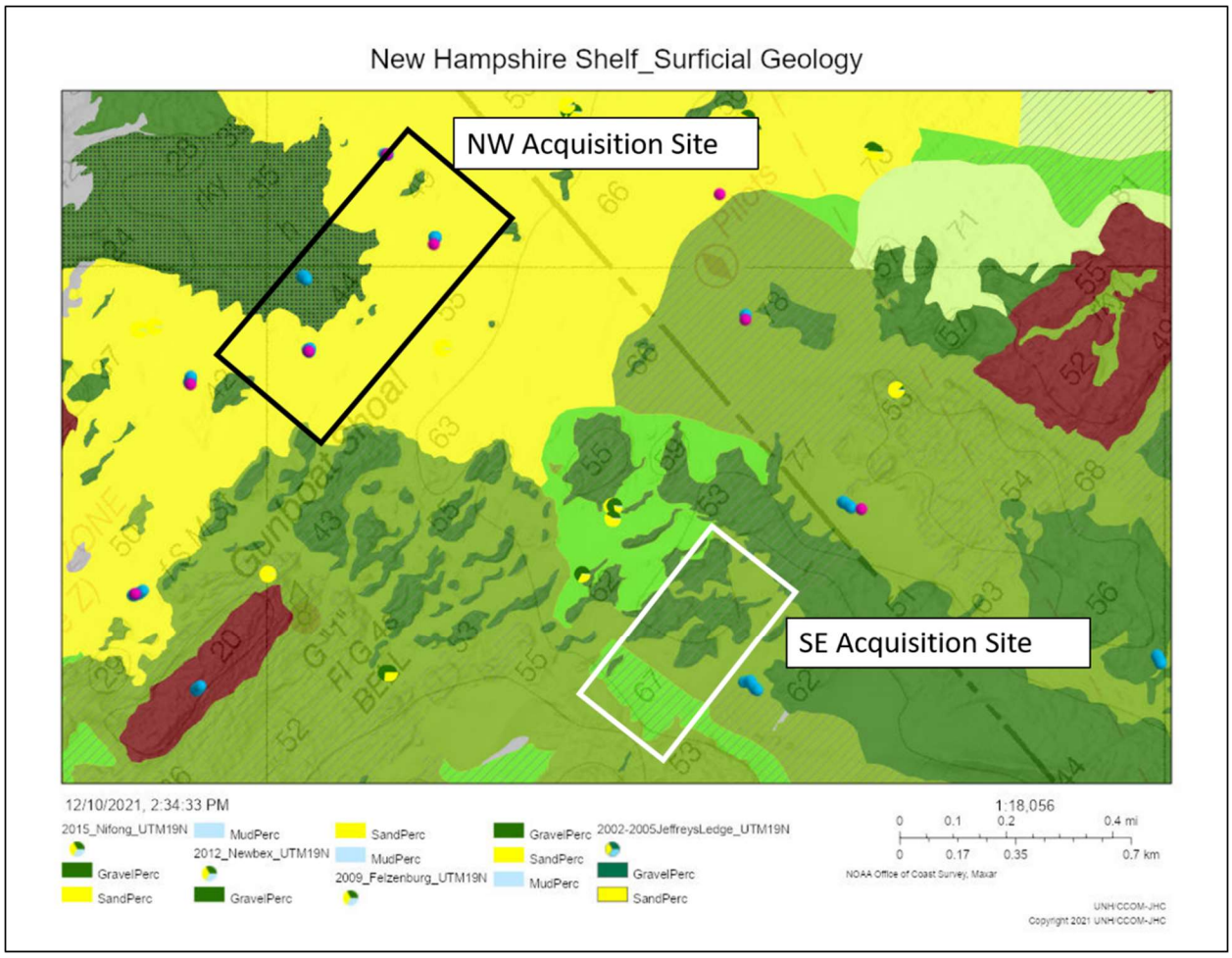

Figure 16: Overlay of seabed characteristics offshore of Odiornes Point. The black box is the NW survey area and the white box is the SE survey area.
(https://maps.ccom.unh.edu/portal/apps/webappviewer/index.html?id=28df035fe82c423cb3517295d9bbc24c# Dec 10, 2021; Ward et al. 2021)

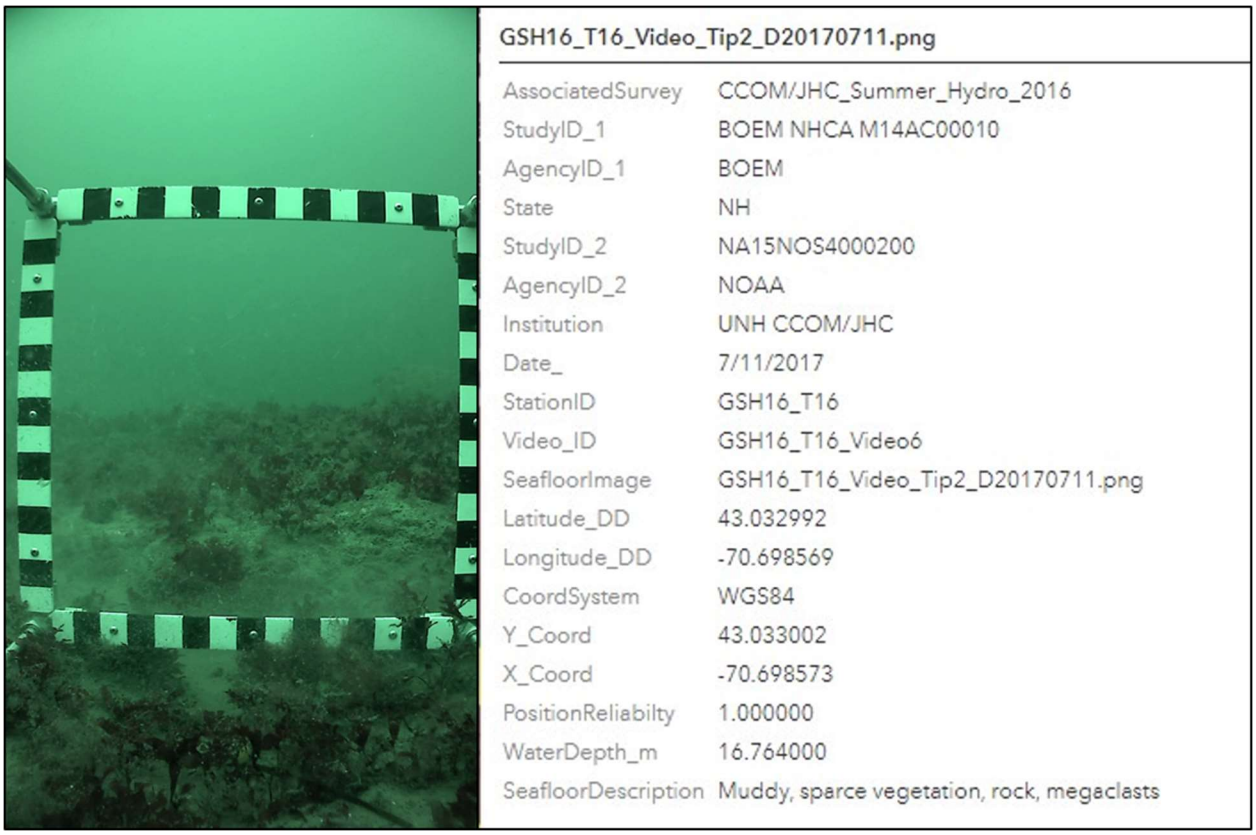

Figure 17: Image from the rocky portion of the NW survey area showing vegetation and the descriptive information for the site. (https://maps.ccom.unh.edu/portal/apps/webappviewer/index.html?id=28df035fe82c423cb3517295d9bbc24c#; Dec 10, 2021)

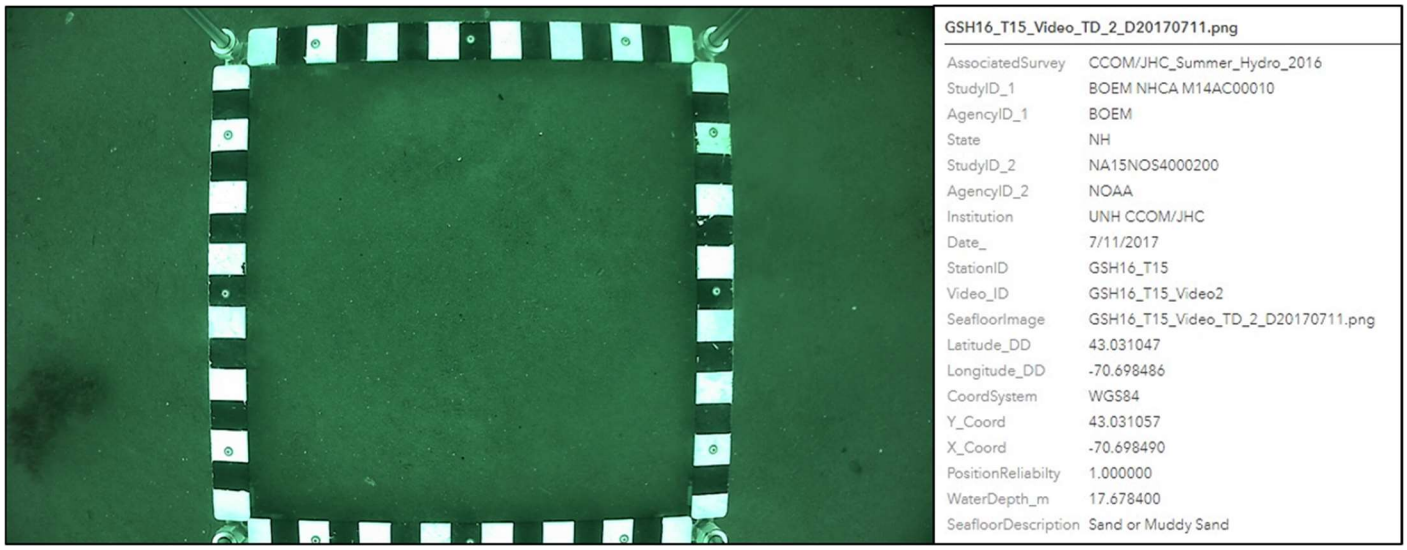

Figure 18: Image from the sand/mud portion of the NW survey area showing vegetation and the descriptive information for the site. (https://maps.ccom.unh.edu/portal/apps/webappviewer/index.html?id=28df035fe82c423cb3517295d9bbc24c#; Dec 10, 2021)

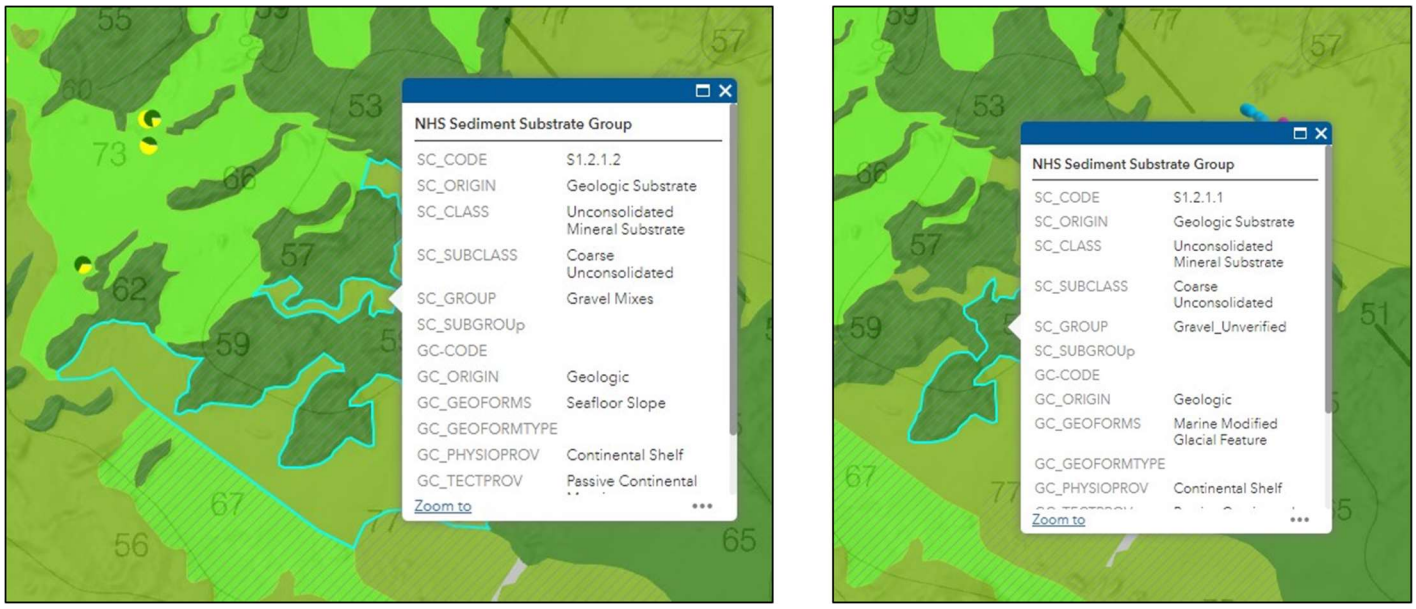

Figure 19: Image from the SE survey area depicting areas of gravel (dark green, right)) and gravel mixes (olive green, left). (https://maps.ccom.unh.edu/portal/apps/webappviewer/index.html?id=28df035fe82c423cb3517295d9bbc24c#. Dec 10, 2021; Ward et al. 2021)

Data Acquisition

R/V *Gulf Surveyor*

The Research Vessel *Gulf Surveyor* (RVGS) is a 48ft aluminum hull catamaran (Fig. 20) built in 2015 by All American Marine in Bellingham, WA. The RVGS propulsion is from twin screws with two geared diesel engines. The RVGS utilizes multiple pieces of deck equipment including a retractable strut, a winch, and an A-Frame, to support various scientific operations. The transducer strut, where the MBES is mounted, is retractable and is deployed vertically through a moon pool that measures ~ 35” x 69 5/16”. The A-frame (Fig. 20) is used for putting various equipment over the stern for deployment or towing and has a safe working load (SWL) of 2000 lbs. For the purpose of this project, an electro-hydraulic winch with 400m of 0.40” Geips armored two cable was installed on the top deck. The RVGS is certified by the U.S. Coast Guard to carry up to 18 passengers, no greater than 20nm from shore (http://ccom.unh.edu/facilities/research-vessels/rv-gulf-surveyor, accessed December 5, 2021).

Figure 20: R/V Gulf Surveyor (http://ccom.unh.edu/facilities/research-vessels/rv-gulf-surveyor).

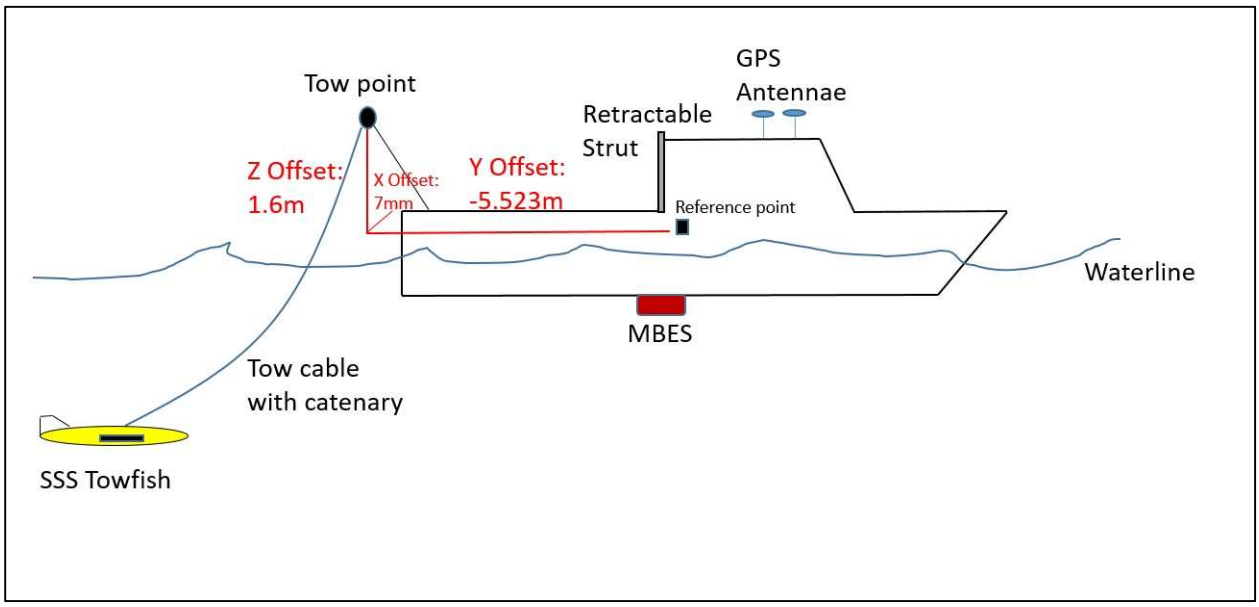

Figure 21: Diagram of RVGS with key locations and the offset of the towpoint to the reference point of the ship (not to scale).

Sidescan Sonar System

For the purposes of this research a Klein 4K-SVY dual-frequency single beam SSS, loaned by Mind Technology-Klein, was employed (Fig. 22). The 4K-SVY operates at 300 kHz and 600 kHz and both frequencies were collected during data acquisition. The lower of the two frequencies matches well with the EM2040P MBES and the ability to frequency match the backscatter imagery played a key role in the

selection of this system and only the 300 kHz data was used for this project. The SSS uses an FM Chirp pulse type with a vertical beamwidth of 50º left and right for both high and low frequency and a horizontal beamwidth of 0.5º for the low frequency, and 0.3º for the high frequency. The sonar also included a dedicated altimeter transmitting at 360 kHz with a depth range of 100m. Data is logged with a time varying gain (TVG) that uses a 30LogR approximation for transmission loss, where R is equal to the range between the SSS and the seabed, with a maximum gain of 48dB. In the 4K-SVY, the sonar data vectors are linear amplitudes that are proportional to acoustic pressure incident on the receive array and are stored as least significant bit (LSB). The sonar is also equipped to compensate for attitude in heading, pitch, and roll. These correctors help to lessen any motion artifacts that may present themselves in the data. By removing the motion artifacts, the imagery is less prone to inaccuracies in intensity.

To provide an improved estimation of position, cable out was fed directly into the acquisition software from the cable counter. This ensured that, along with the lever arm offsets, the layback calculations were done in near real-time during acquisition.

Figure 22: Klein 4K-SVY Sidescan on deck of the R/V Gulf Surveyor with tow cable installed.

During testing in advance of the project data acquisition, the SSS was inadvertently run aground and suffered minor damage to the nose cone.Upon examination by the manufacturer, it was their assessment that no significant errors were introduced into the system and resulting data from the grounding.

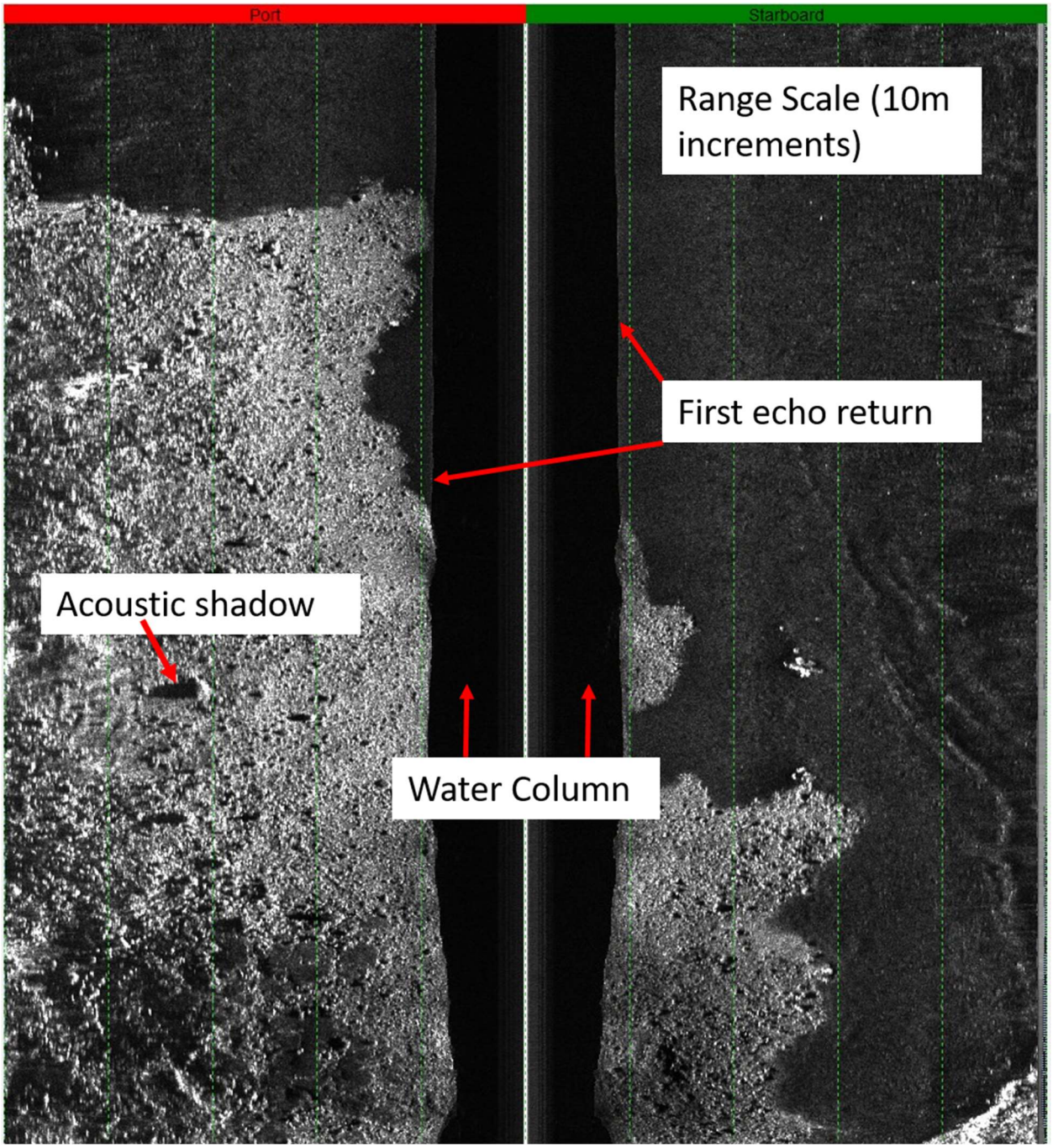

Figure 23: Example of typical SSS data with acoustic shadows, range scale, first return, and water column.

Multibeam Echosounder System

The MBES system used was a Kongsberg EM2040P on loan to CCOM from Kongsberg. The unit seen in figures 24 and 25measures 414 x 298 x 166 mm (L x W x H) and weighs approximately 20kg dry and 4.7kg when submerged. The EM2040P operates at frequencies of 200, 300, 400 kHz with the option of having 600, and 700 kHz frequencies for high definition as well. For this research, the sonar was operated at a nominal frequency of 300 kHz. Operating at 300 kHz, the sonar employs a continuous

wave (CW) transmit pulse, with a pulse length of 19-324µs and a beamwidth of 1.3º x 1.3º. The system parameters used for acquisition followed optimal bathymetric data collection standards of swath angles at 65º from nadir on port and starboard, dynamic yaw stabilization enabled and the system was run in a high definition equidistant, multi-sector and single (??? Really – could have sworn it was dual) swath. These parameters are typical of NOAA MBES operations and are described in the Kongsberg Seafloor Information System (SIS) operating manual (Kongsberg 2021).

Positioning was fed directly to the EM2040P from an Applanix POS MV V5 with Trimble OmniSTAR GNSS precise point positioning (PPP) to provide real-time position and motion stabilization. Surface sound speed from an integrated sound speed sensor (Fig. 24) was sent in real-time, and additional sound velocity casts were taken periodically to ensure proper spatial and temporal distribution throughout the survey area.

The EM2040P is installed on a rigid, center-line mounted strut on the R/V *Gulf Surveyor*. This mount is capable of being raised and lowered and when in the lowered position, the offsets are precisely known so as to put the sonar in the correct vessel reference frame (Fig 25).

Figure 24: Kongsberg EM2040P MBES with Integrated Surface Sound Speed Probe. (https://www.kongsberg.com/maritime/products/ocean-science/mapping-systems/multibeam-echo-sounders/em-2040p-mkii-multibeam-echosounder-max.-550-m/)

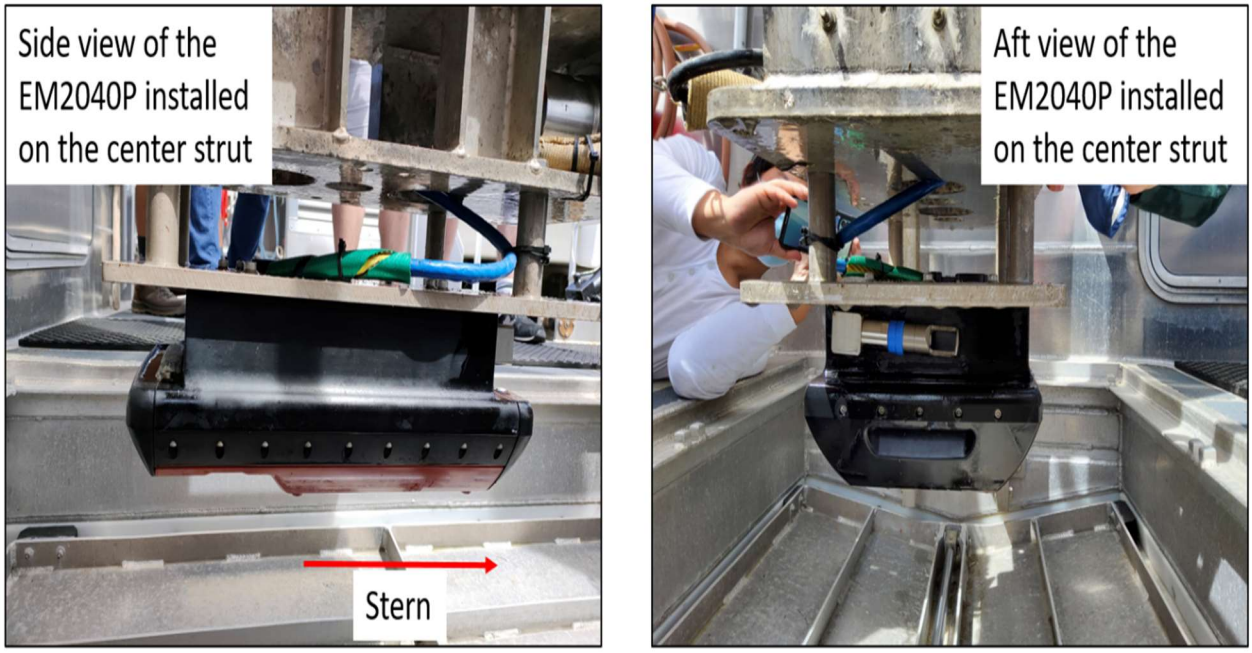

Figure 25: EM2040P as installed on the center strut of the R/V Gulf Surveyor (Photo: Lt. Patrick Debroisse, NOAA).

System Calibrations

For NOAA hydrographic surveys, the Office of Coast Survey Field Procedures Manual (FPM) states that it is good practice to perform a calibration test on the systems being used prior to the beginning of a field season, when a new piece of survey equipment is installed, or has been moved for any reason. These tests, commonly referred to as “patch tests”, quantify the uncertainties in the timing (latency), heading, pitch, roll, and yaw of an MBES measurement. The acquired data is then used to analyze each error parameter individually (FPM 2021), and the corrections are applied directly into the data acquisition software.

For a SSS system, the FPM suggests that the sonar should be able to detect an object with dimensions of 1m x 1m x 1m. The position accuracy of the targets detected by the SSS need to be good enough for the target to be located to have the least depth and position determined through other methods, generally an MBES, or diver investigations (FPM 2021). There are no corrections applied to the SSS data, and thus the SSS patch test is considered more of a “confidence check” than a calibration.

Prior to data acquisition, the SSS and MBES systems had standard patch tests conducted and MBES offsets applied. A set of lines were laid out for the SSS such that it could be determined, with

confidence, that the system was capable of detecting targets and that the positioning of these targets was acceptably accurate when referenced to the MBES data (Fig. 26). A target area was selected using previous data, and the target position was taken from concurrently collected MBES data for precise positioning. The calibration test was conducted using a 50m SSS range scale. The criteria for the positioning test is that, with a 95% confidence, any future measurement will not give a positional error greater than 10m for a towed configuration (HSSD 2021). By using a mean radial distance of the SSS positions in relation to the position of the MBES target, the 95% confidence error (sample mean + 1.96* standard deviation) in this patch test is 7.9m and therefore passes the confidence check. The distribution of the targets, prior to map correcting, in a geographic frame and in a ship reference frame can be seen in figure 28. Appendix I contains the spreadsheet used to calculate the errors.

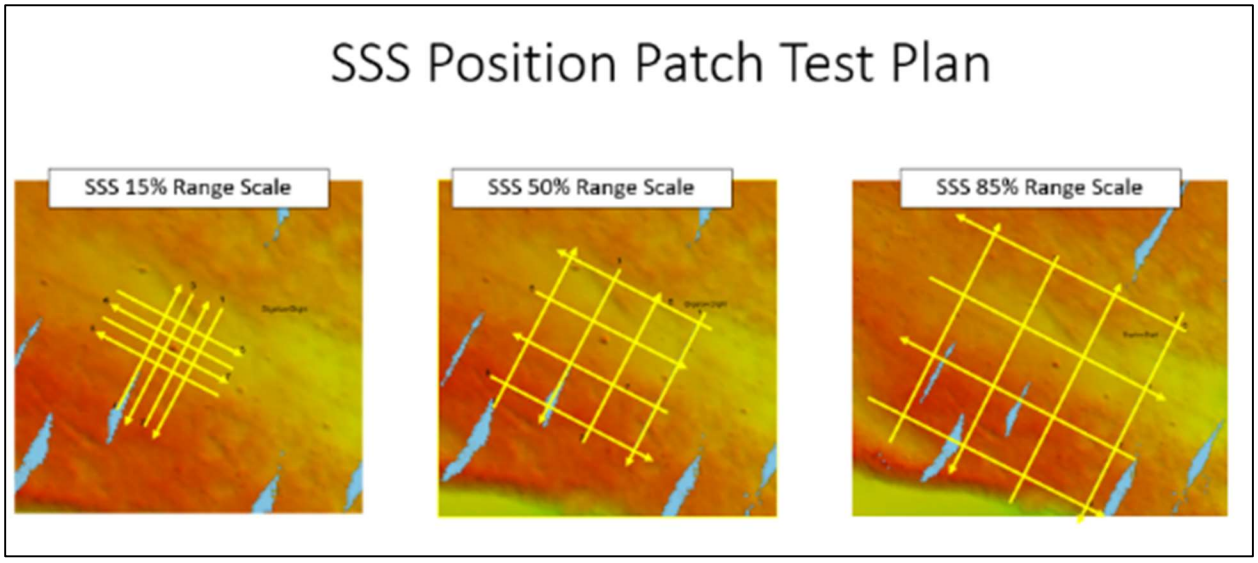

Figure 26: Layout of SSS Lines for Position Confidence Checks at a 50m range scale.

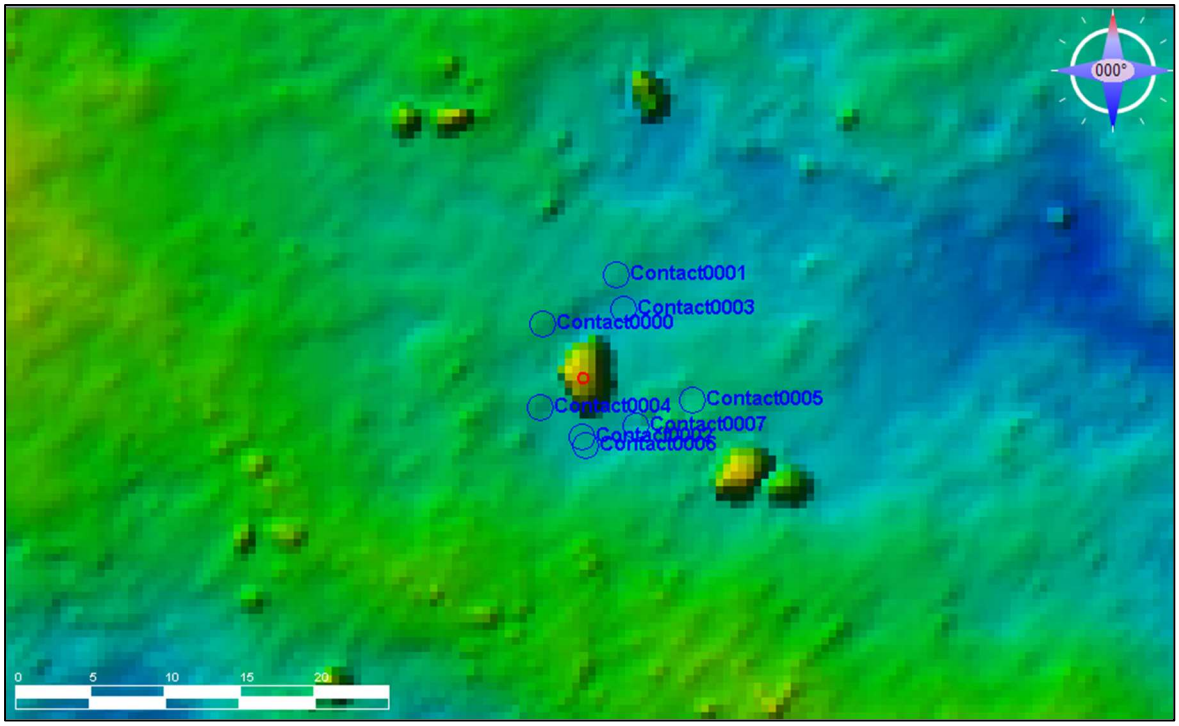

Figure 27: SSS contact positions (blue) in reference to the MBES target position (red).

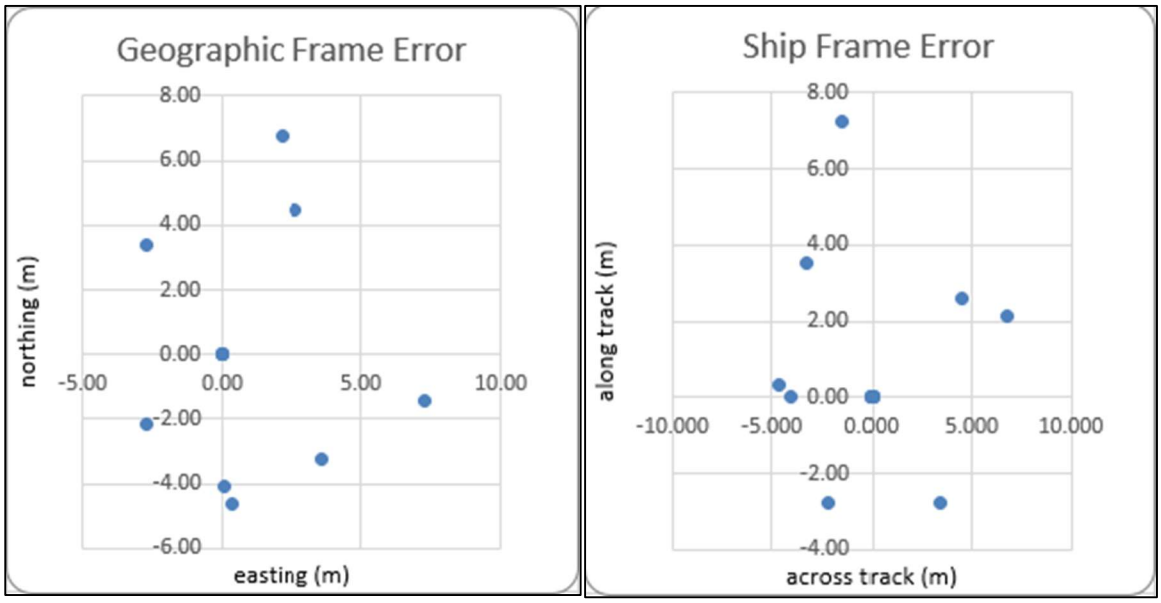

Figure 28: Contact position errors in a geographic reference frame and in the Ship reference frame. Contact positions are predominately to the East of the MBES position.

To test the initial capability of the Map Corrections function in *SonarWiz*, the MBES feature was used as a reference point and the feature positions were again selected in each individual SSS data file. The positional offset was then utilized by *SonarWiz* to adjust the navigation of the corresponding line (see detailed explanation below). As can be seen in the results below, the tool worked extremely well

and reduced the error uncertainty at the 95% confidence level to 1.1m using a mean radial distance and 0.5m using the method described in the FPM of 1.96*RMS standard deviation.

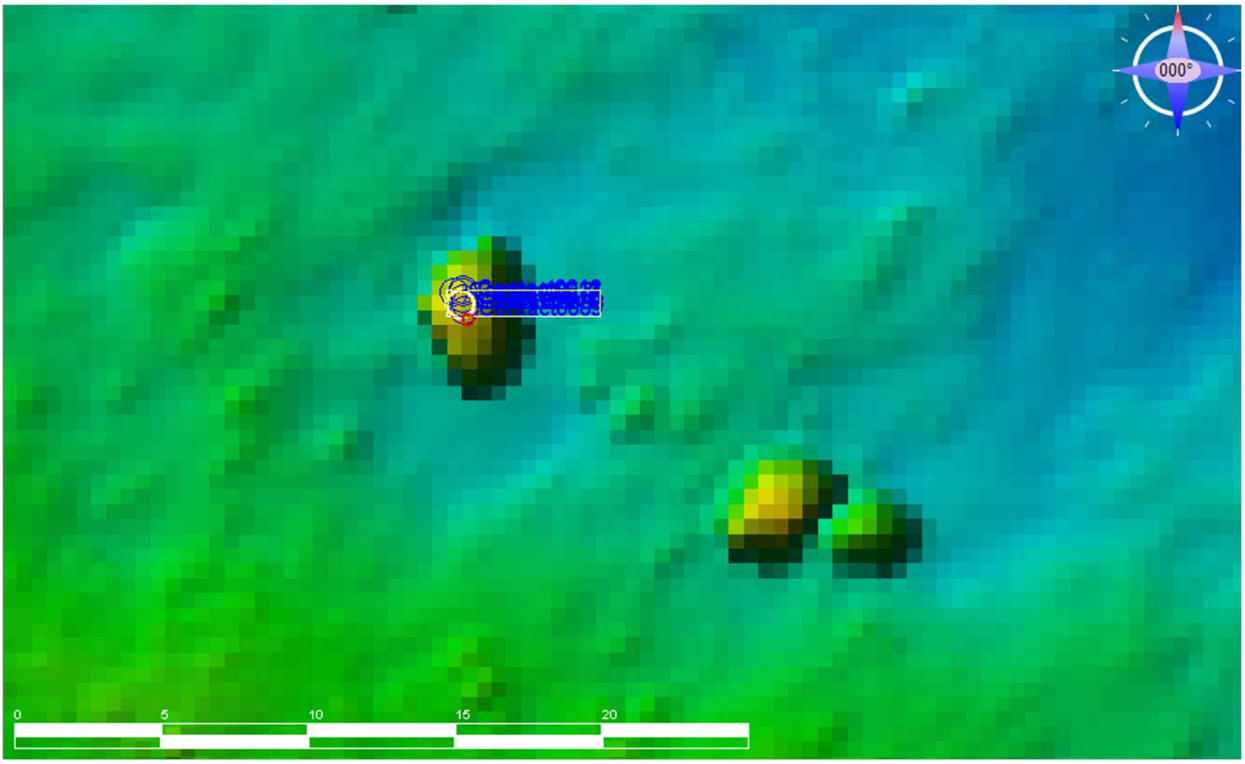

Figure 29: SSS contact positions post application of Map Corrections.

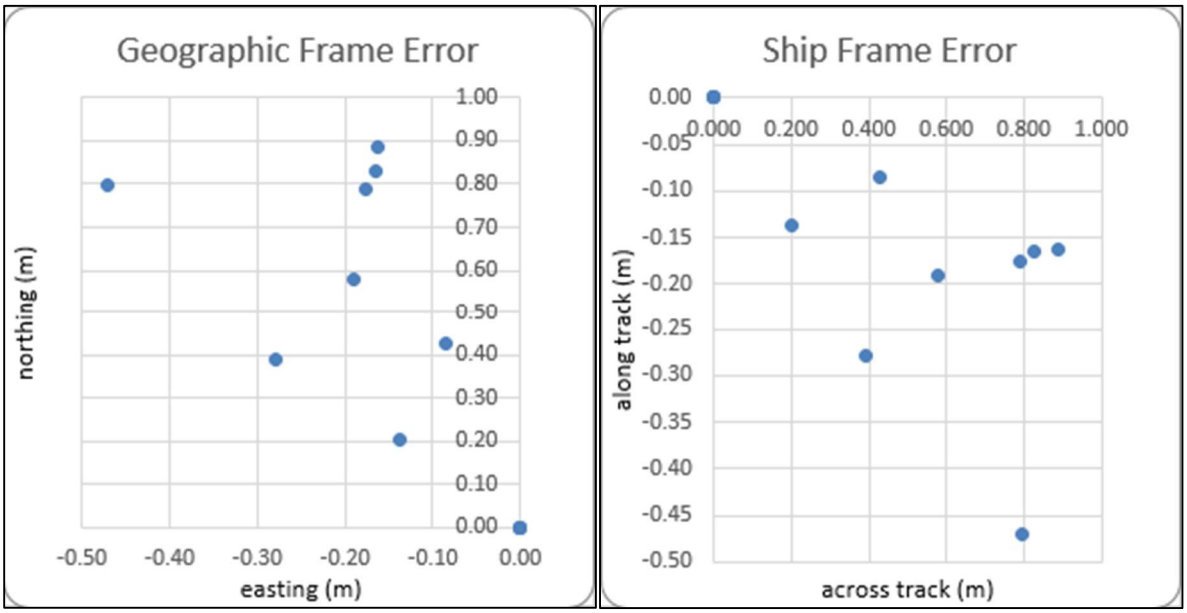

Figure 30: SSS contact positions seen in a Geographic and Ship reference frame post-application of Map Corrections

Data Acquisition

Post calibration, the data collection followed a plan such that lines were spaced 60m apart for SSS acquisition at a 50m range scale, and 80m apart for a 75m SSS range scale (Fig 31). This ensured that

there would be sufficient overlap of the outer beams to allow for a seamless SSS mosaic and proper characterization analysis. In the NW site, lines were run so that there were two independent sets of data that would equate to 200% SSS coverage as would be used for a NOAA Object Detection survey. Each set of lines provides 100% SSS coverage of the area and were mosaicked independently of each other.

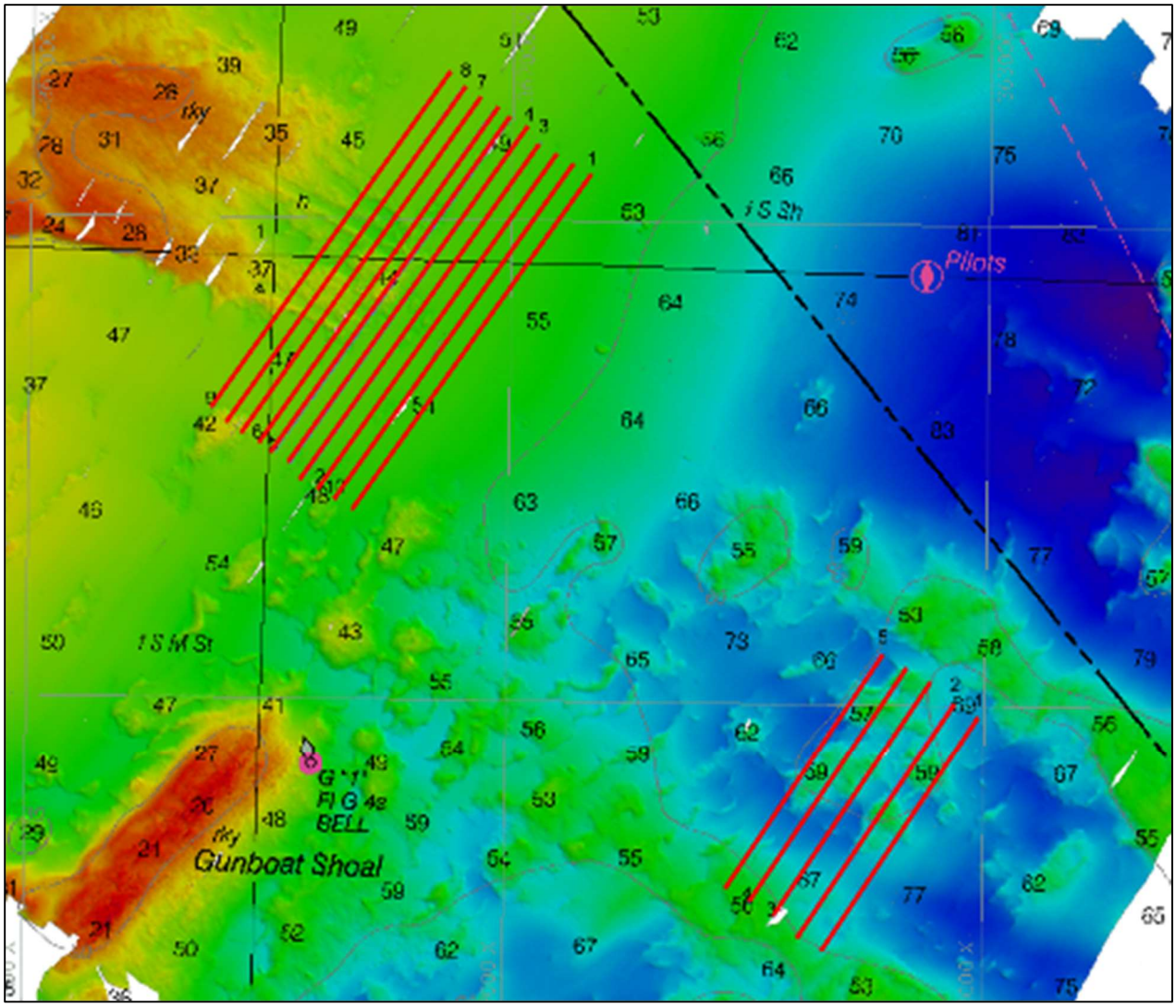

Figure 31: Survey area with 60m and 80m line plans shown in red.

Data Processing

Sidescan Sonar

The SSS data were processed in Chesapeake Technology S*onarWiz* software. The processing procedures followed standard workflows where the SSS data were imported and checked for any spurious navigation and altitude errors. Upon import, the position of the SSS data is taken from raw files

where Klein uses the cable out and fish depth to calculate the layback and store the position as "layback_lat/lon". To project the heading of the towfish, two options are available in SonarWiz. The user can select either "Sensor Heading" or "Course Made Good". Sensor heading takes the raw heading data from the input file, which may differ greatly from the actual direction of travel. For the purpose of this project and upon the recommendation of Mind Technology, the data were projected using course made good (CMG) which adjusts the navigation of the towfish to align with that of the ship in the along-track orientation. The CMG heading projection is derived from the raw position data and a time constant that is used for course smoothing, in this case, the default constant of 300 pings was used.

Two methods of mosaicking were examined, shine through and cover up. For the purpose of this research, the "shine through" method of SSS data mosaicking was used. In this method, the data with the greatest amplitude value is used as the observable pixel when overlapped with another line that occupies the same location (Chesapeake Technology 2016). This allows for a more seamless mosaic than other methods such as cover-up where each line is displayed in the order drawn and no averaging occurs. The other benefit of shine through is that contacts are captured whereas with cover up, they may be obscured if not present in the overlapping line, or offset and displayed multiple times (Fig. 32)

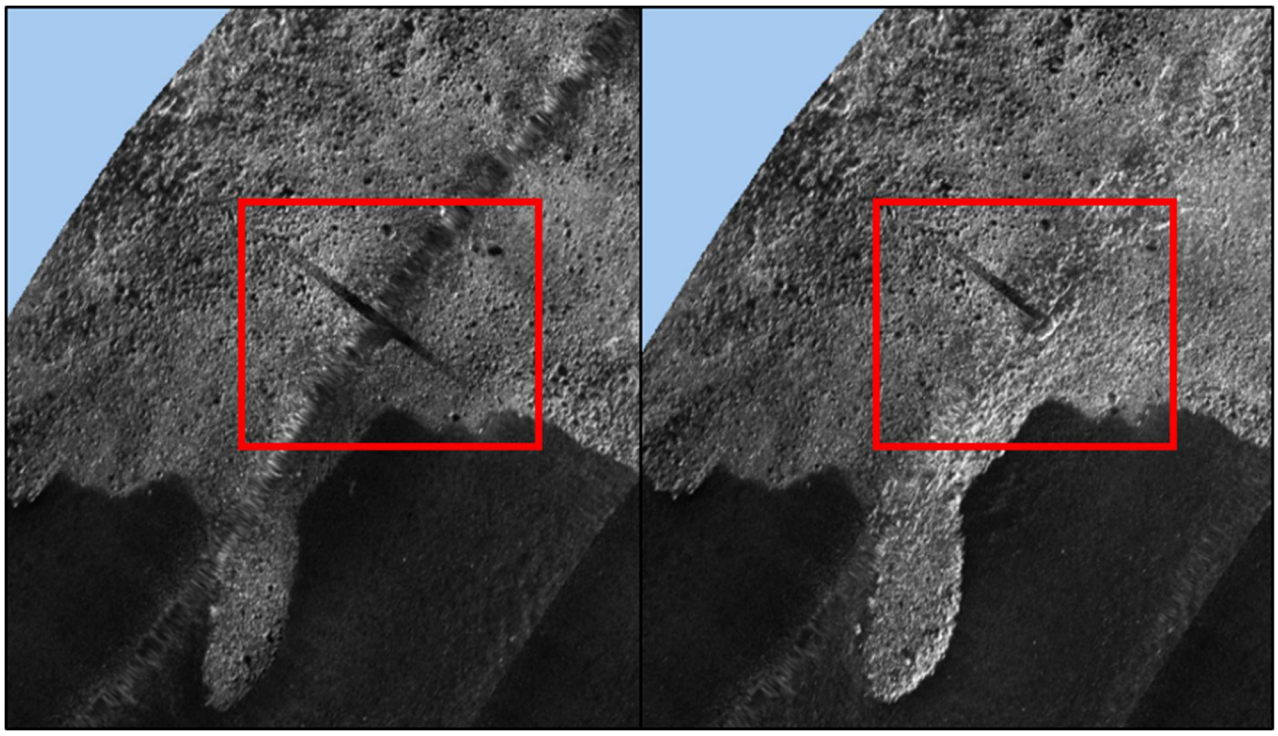

Figure 32: Cover Up mosaic (left) hiding contact vs. Shine Through mosaic (right) showing contact.

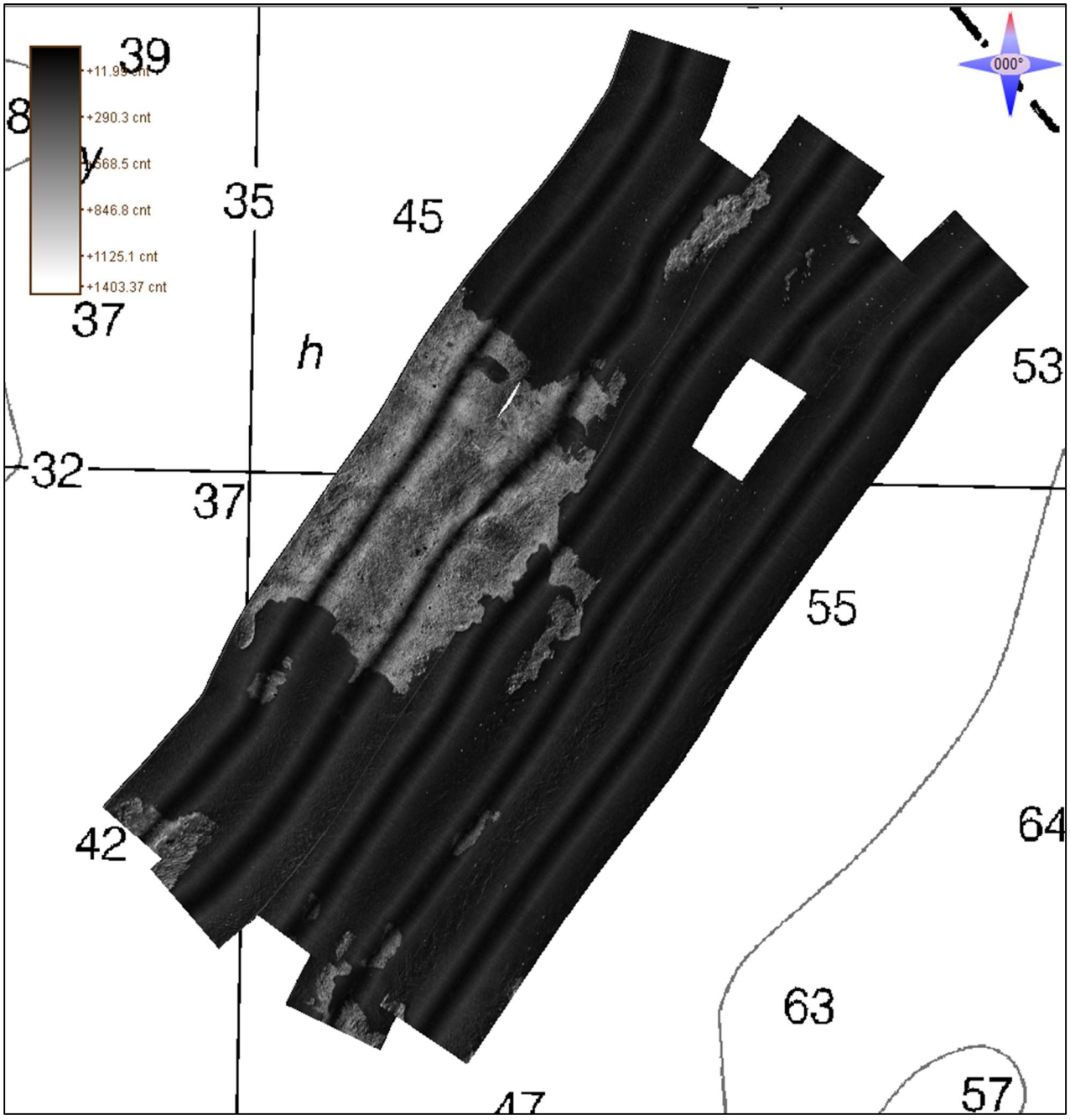

Figure 33: SSS mosaic showing all lines prior to having gain and positioning corrections applied, using Auto-All Data. Overlaid on RNC 13283.

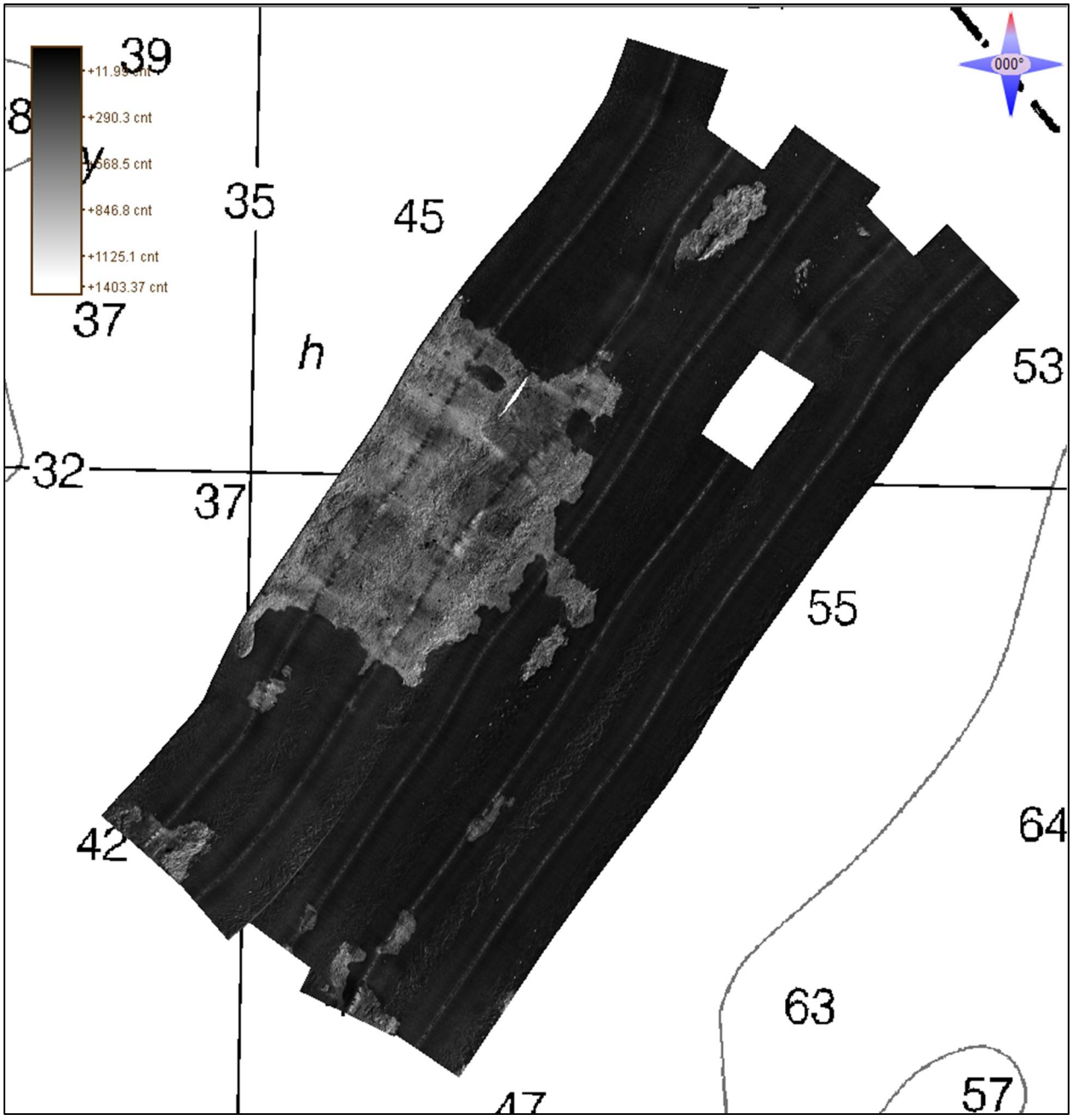

Figure 34: SSS after having Map Corrections and EGN applied with the Auto-All Data visualization.

The values associated to the gray scale are dependent on the data type, in this case, Sidescan Ch. 1 and 2 (Low Frequency). The range of display can be set to Manual, Auto - This Data, and Auto - All Data. For the purpose of this research, the "Manual" mode was selected. This allows the user to adjust the gray scale across the entire mosaic.

Multibeam Echosounder

The MBES data were processed in QPS Qimera software. The data were imported in the raw .kmall file format that is native to the Kongsberg EM2040P data acquisition system. Sound velocity

profiles were applied in real-time during acquisition. Though some refraction can be seen in the data at the outer beams prior to filtering, the vertical offsets due to the refraction are minimal (~10cm) and no refraction artifacts are noticed after filtering (Fig. 35). Any refraction artifacts seen would most likely have been mitigated by collecting more sound velocity profiles, but the offsets were not deemed significant for the purposes of this project.

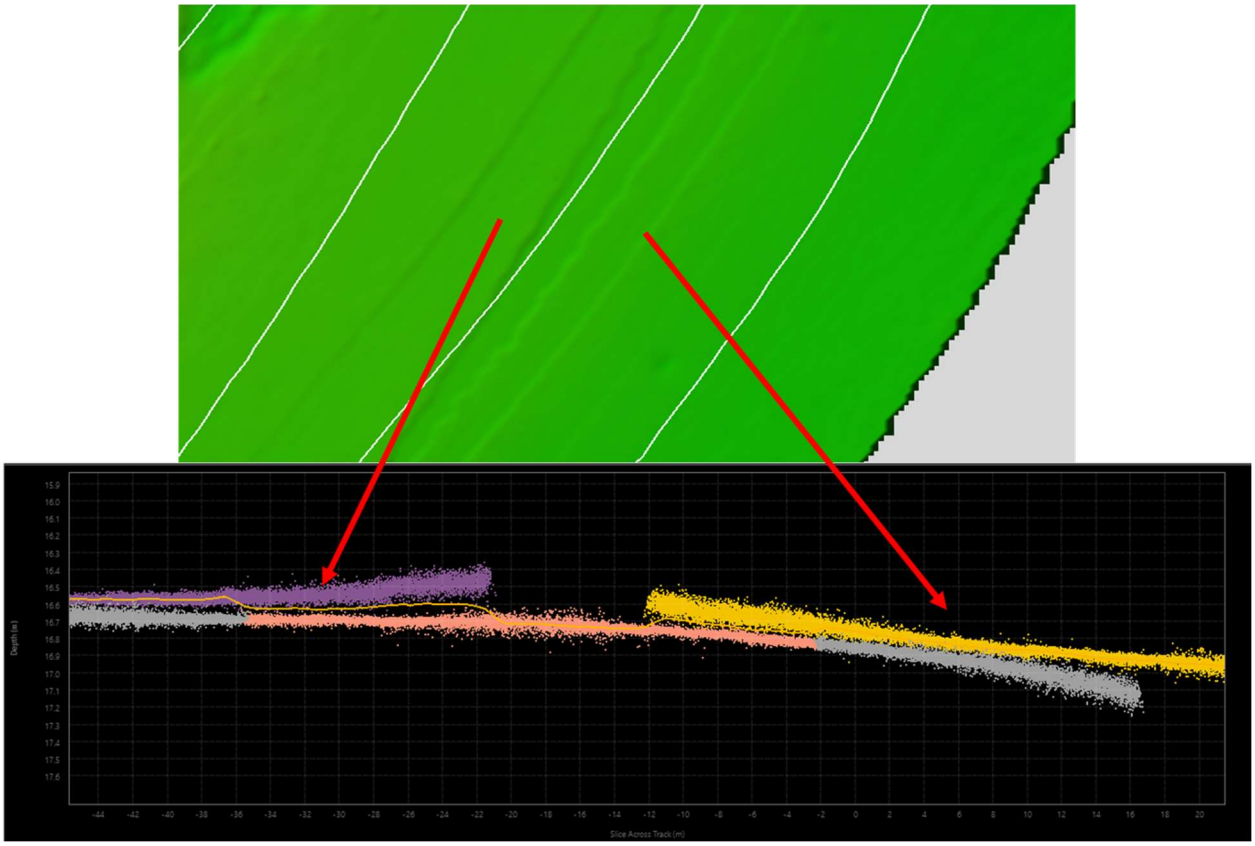

Figure 35: DTM (top) showing refraction artifacts and the same artifacts as seen in the ping data (bottom).

After import, the data were transformed, as they would be in a traditional NOAA survey, from the ellipse to chart datum using a grid created in the VDatum SEP from Shapefile tool, which is a product in NOAA's open-source software Pydro (https://svn.pydro.noaa.gov/Docs/html/Pydro/universe_overview.html, accessed 12/1/2021). By creating a Shapefile (.shp), this can be used to create 100m resolution grid. This grid is then used to perform the vertical transformation from the ellipse to chart datum with the vertical uncertainty outputted by the program.

Once the data had been fully imported and processed, a digital terrain model (DTM) was created using the Combined Uncertainty Bathymetric Estimation (CUBE) algorithm at a 50cm resolution. As run, the MBES lines show coverage that is approximately 80% of the SSS swath (Fig. 36). To better simulate very shallow water surveys, the MBES lines were then filtered to 45º off nadir on both port and starboard (Fig. 37). The filtered DTM shows only the set of lines that were used for data analysis.

For the purpose of using these grids in other software packages, they were exported to a floating point geotiff, which allows them to be used in most GIS applications. The processed data were also exported to GSF (Generic Sensor Format) for use in QPS FMGT to process the acoustic backscatter.

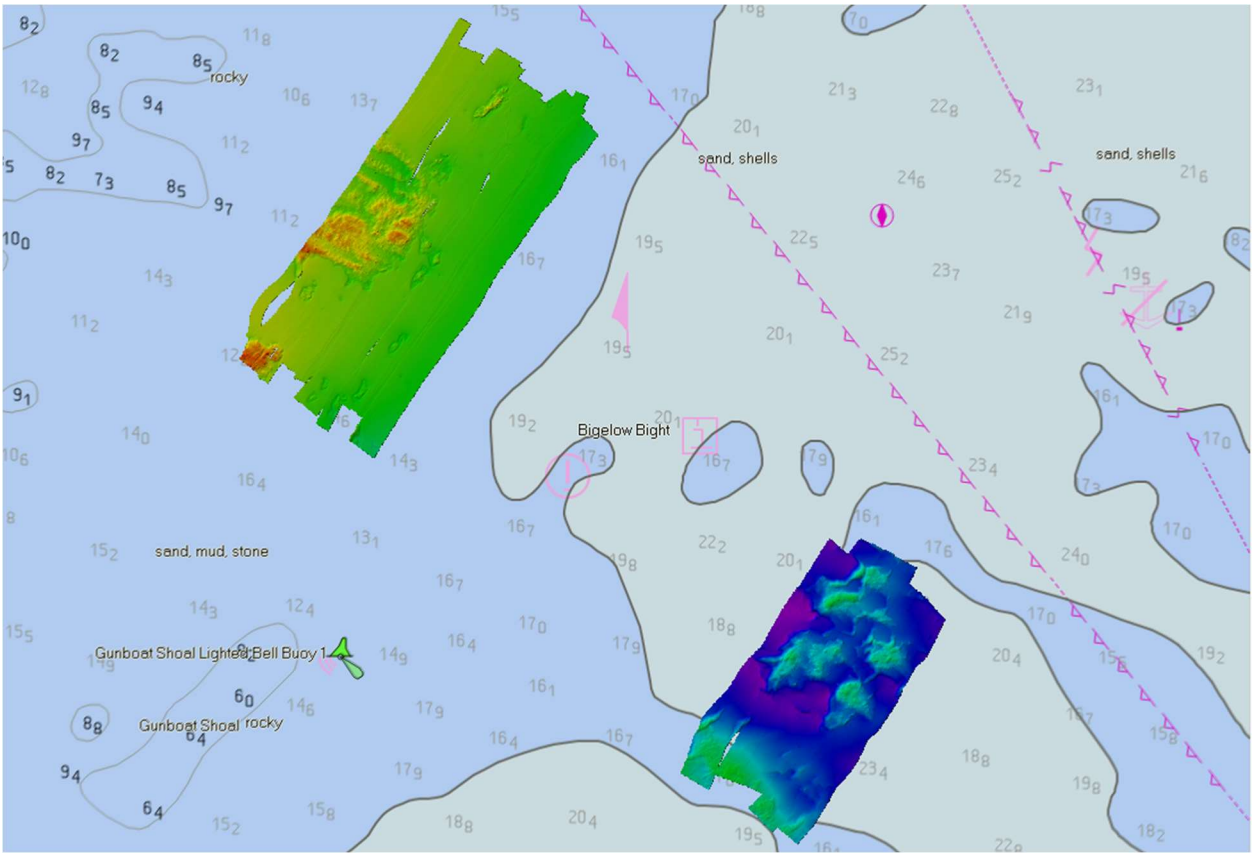

Figure 36: Full Coverage DTM of EM2040P MBES Data.

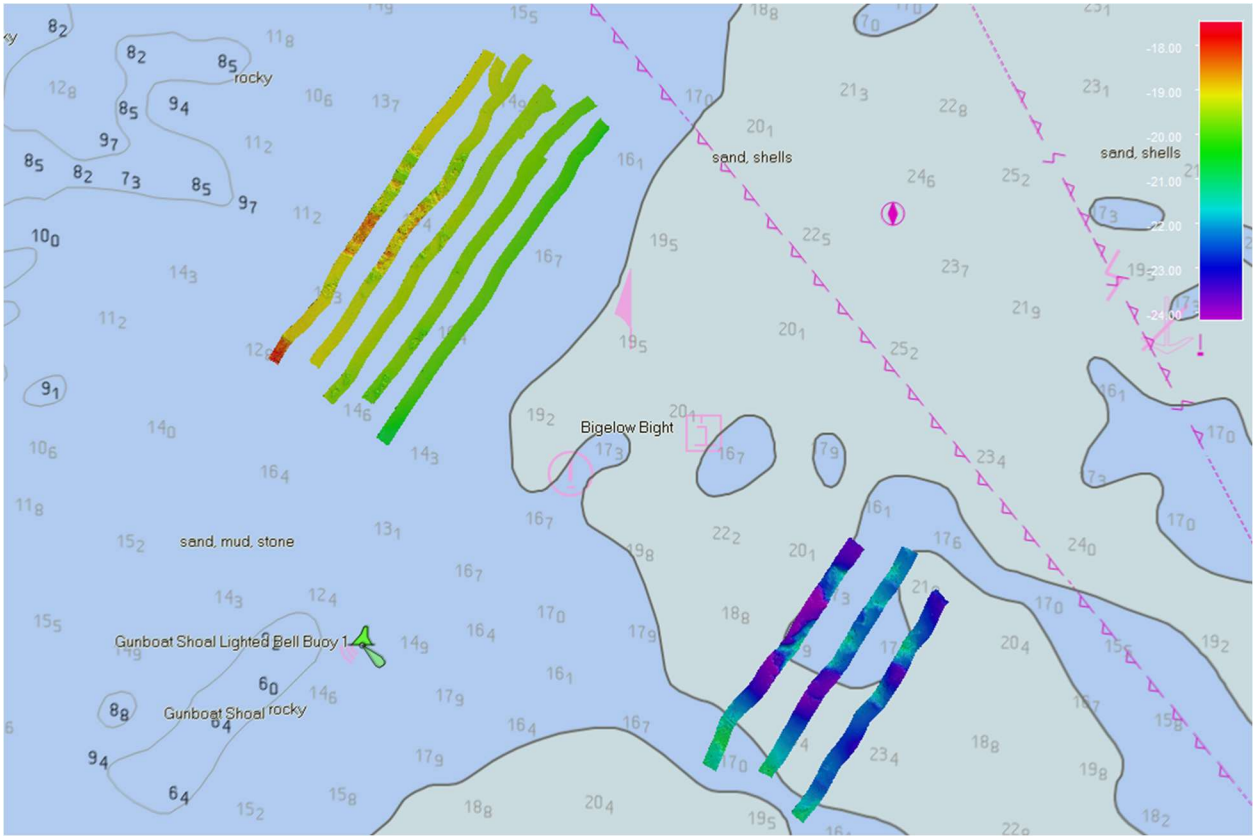

Figure 37: DTM of EM2040P data after being filtered to 45º from nadir.

Multibeam Acoustic Backscatter

To create the MBES backscatter, the data were processed in QPS FMGT. The GSF files that had been exported from Qimera were imported into FMGT and a mosaic resolution of 50cm was chosen to match the resolution of the SSS imagery. The backscatter data measurements output by Kongsberg EM mutlibeams are first order estimates of the bottom backscatter strength (Hammerstad, 2000). The EM2040P data is automatically adjusted for factory-estimated source level and receiver gains, and the Qimera software does a first order flattening of the mean angular response. As a result, the data should be largely independent of grazing angle and should represent the typical range of expected seabed backscatter strengths that vary from ~ -5 dB (a gravel/rock) to – 30 dB (fine sands and muds).

The backscatter was exported in separate mosaics for each area at the default range of -10 to 70db (Fig. 38). A second mosaic of the NW site was exported after visually approximating the intensity from the SSS imagery. The second mosaic shows a range of -4 to -28db (Fig. 39). The range displayed in the grey represents the backscatter strength in decibels. The lighter shades represent higher intensity from “hard” seafloor, or that with a higher reflectivity, and the darker shades represent lower intensity

from “soft” seafloor or that with a lower reflectivity. The default recording and display range is 10 to -70db (notably extending well below expected seabed backscatter strength values) when processed in QPS FMGT.

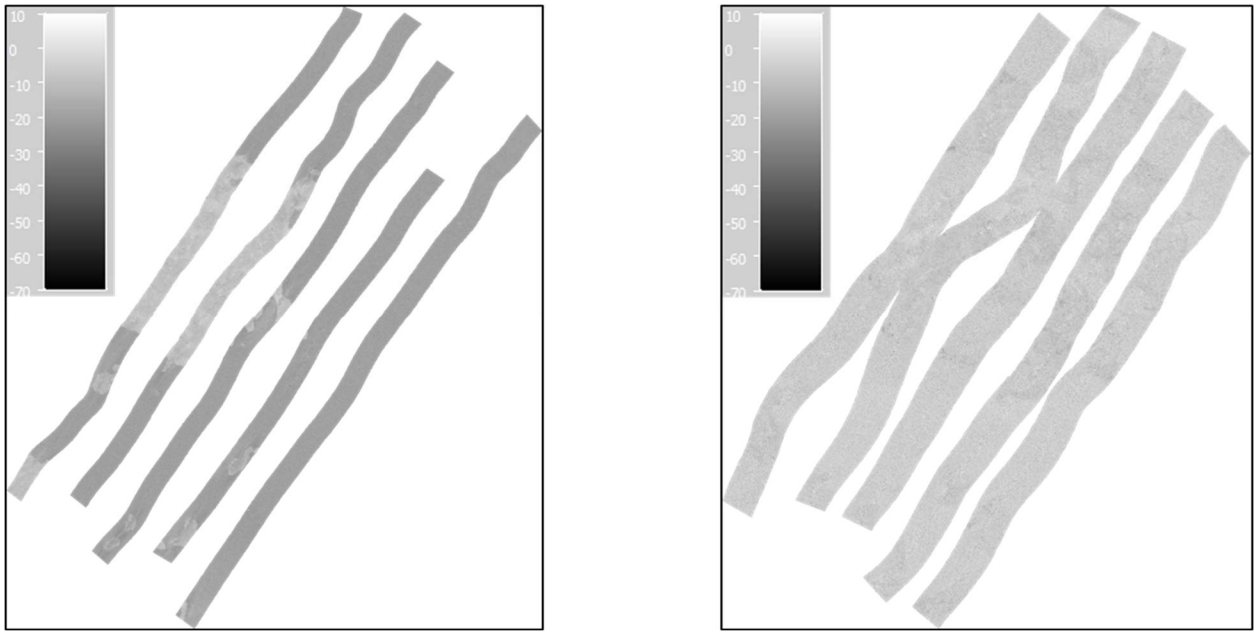

Figure 38: MBAB collected by EM2040P at 300 kHz with a 50cm resolution. The NW acquisition site is on the left and the SE acquisition site is on the right. Backscatter intensity is represented in decibels at the default scale of 10 to -70dB.

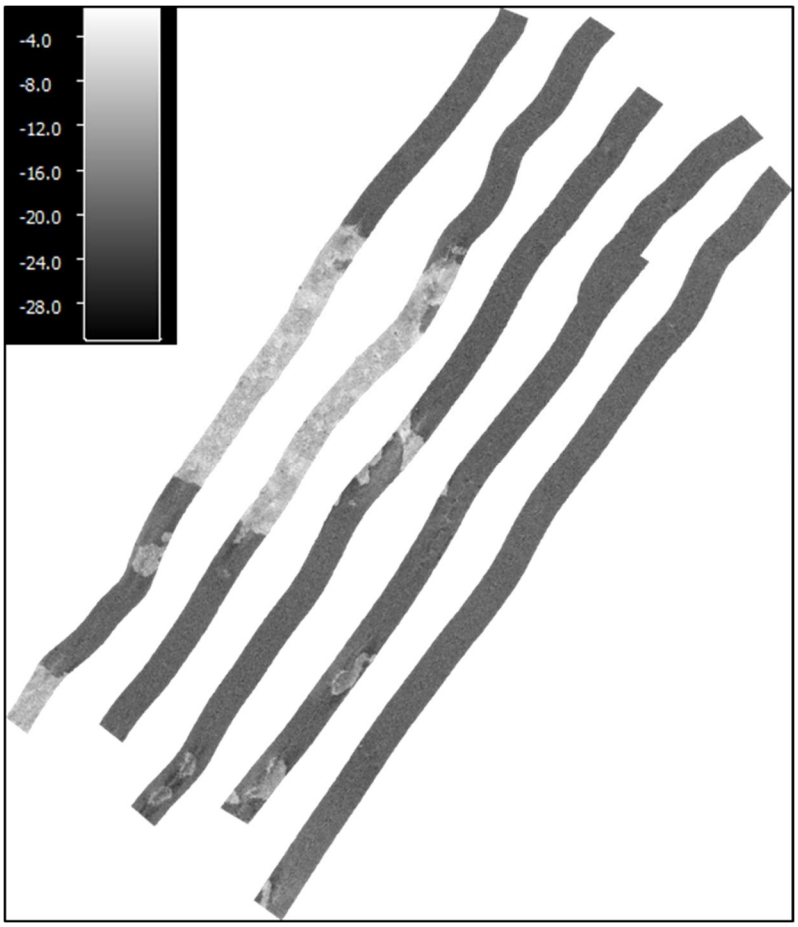

Figure 39: The NW MBES data after being adjusted to show a visual range of -4 to -28db.

Data Analysis

SSS and MBES Positioning Correlation and Analysis

To compensate for any position anomalies that exist between the SSS and MBES data, a process similar to cartographic rubbersheeting (Blondel 2009) (but operating on the data itself, not the image), called Map Corrections was applied in SonarWiz. This process takes the assumed "true" position of a contact from the MBES data and the position of the same contact in the SSS data and adjusts the actual navigation in the SSS to match that of the MBES. This process works by adjusting the entire SSS image and not just the target position. The process can adjust each line of SSS data individually, or use map correction points from all lines. Chesapeake Technology recommended to use the option of using map corrections from the same line. In figure 40 below, the image on the right shows the initial ("bad") position of the SSS contact (blue circle) and the "true" position in the MBES base map (white box). The distance between the two points of reference is approximately 9.7 meters. In figure 41, the blue marker represents the MBES position and the green marker represents the original SSS contact position. As can be seen, the SSS and MBES positions are now collocated. Figure 42 shows another example of pre and post Map Corrections. On the left, it appears that there are two separate lines of lobster traps. After applying Map Corrections to both SSS lines, independent of each other, the image on the right now shows that there is only one array of traps.

The positioning corrections in the SE data site proved to be slightly problematic. Each line was corrected to match the corresponding MBES data, but the NW-most SSS line and the center SSS line do not match up precisely with each other (Fig. 43). This is evident when looking at the area in the South where there are strong sand waves present. Multiple map corrections were made with both lines, with the best estimate of position ending up at approximately 7.5m between the two lines.

As shown with the SE site, the issue that arises due to the nature of this type of survey is that with a relatively narrow swath of MBES data, there may not always be a point of reference to use for

correction. This is even more so if surveying in areas that are relatively featureless such as some regions in the Arctic or Gulf of Mexico. In such regions, a reference target could be deployed in the survey area for registration, but if no salient features are present in the survey area, the need for swath adjustment is actually less compelling. By having more points of reference, one can better correct the position offsets of the SSS data. For the purpose of this research, I specifically chose not to use any of the overlapping MBES that did not directly correspond to the SSS data was being analyzed.

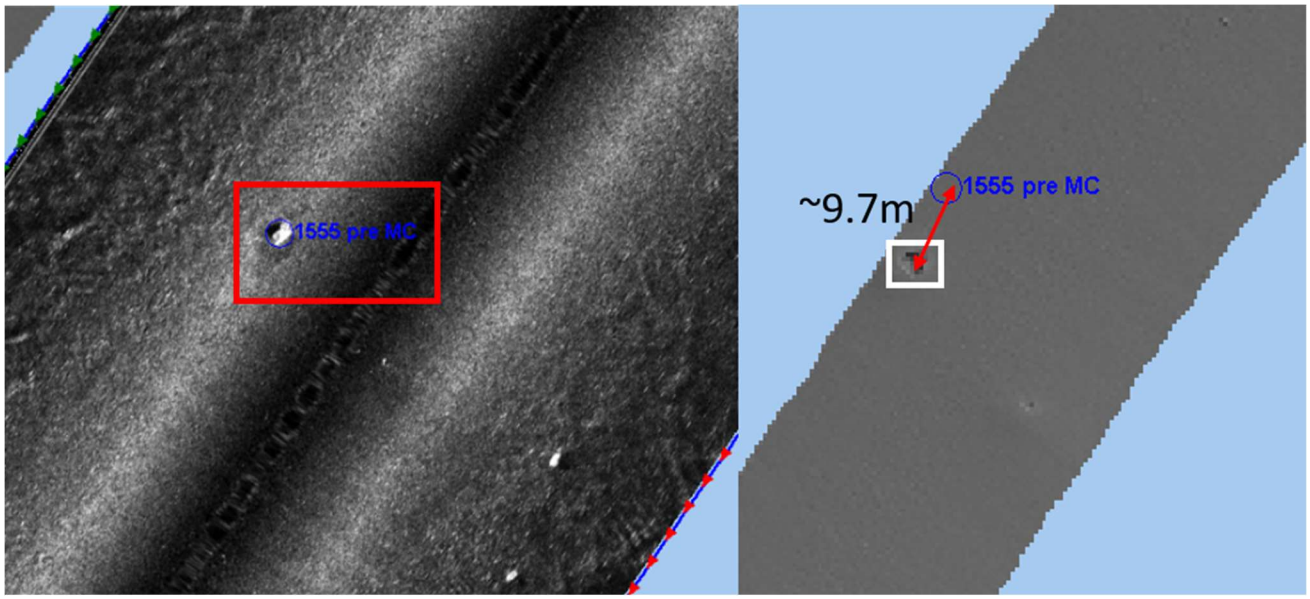

Figure 40: SSS contact position (left) and assumed "true" position from MBES (right).

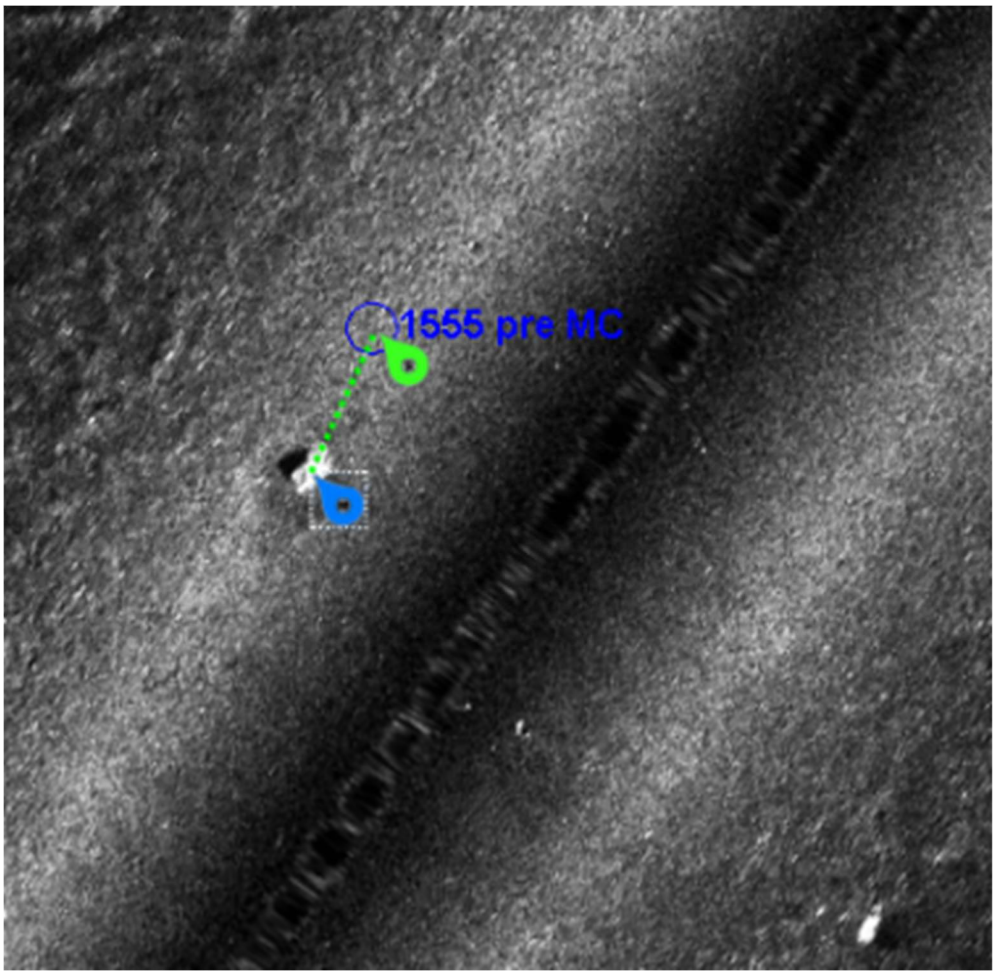

Figure 41: Position of SSS contact after having the Map Correction applied. Original SSS position annotated with green marker.

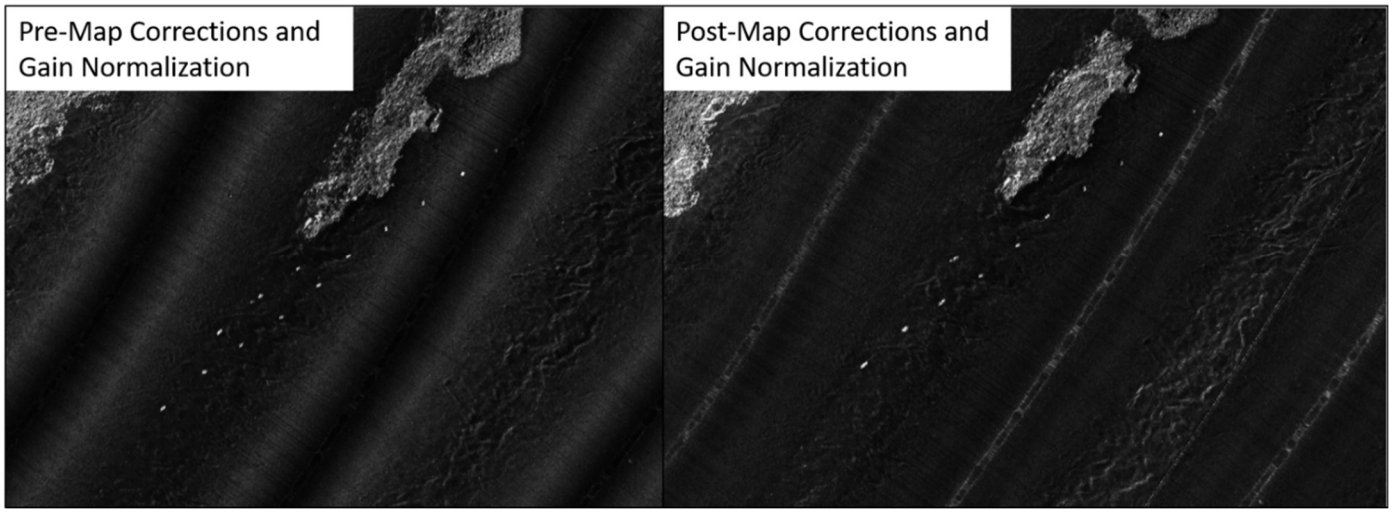

Figure 42: Another example of Pre (left) and Post (right) Map Corrections showing what initially appears to be two separate lines of lobster pots.

Figure 43: Disparity of ~7.5m between two SSS lines after having Map Corrections applied. The red box highlights the area where the sand waves should overlap.

SSS and MBES Backscatter Intensity Analysis

Once all the map corrections to the SSS were applied, the GeoTiff from the MBES acoustic backscatter (MBAB) was imported into *SonarWiz* for comparison. Figures 44 and 45 show each data type as standalone images from both survey areas, prior to being combined. The MBAB was initially adjusted in *FMGT* to provide a best match to the SSS imagery and then using the MBAB as a reference, the SSS mosaic was adjusted manually to achieve as near a visual match as possible (Fig. 46). When using the Manual adjustment, the minimum and maximum color values are stretched across the mosaic linearly (Chesapeake Technology 2021). Blondel (2009) describes this method in detail.

While this method of qualitative analysis provides a visually meaningful product, without being able to conduct a quantitative comparison of the SSS intensity values to the MBES backscatter, a definitive result of the qualitive backscatter intensities cannot be established. An improved approach would be to convert the linear amplitude values from Klein to 10xlog intensity values in order to switch to a dB range. Then the only qualitative step would be an arbitrary offset, notably without needed to guess the dynamic range.

The MBES backscatter geotiffs are exported with the amplitude in the Z-value as decibels, which allows the user to see the value when hovering pointer over a given position, depending on the software being used. For the SSS mosaic, when exported from SonarWiz, this option is not available. Other software packages do include a Z-value intensity, sometimes as decibels, when exported as a floating point geotiff. This makes a quantitative analysis much more practical when comparing SSS intensity with the MBES backscatter.

The ability to match the two data sets was easier where there were boundaries of high and low backscatter intensities and thus greater available dynamic range in the observations to estimate the linear stretching needed. Areas where the intensities appeared homogeneous, such as the SE survey site, proved more difficult than the NW survey area to normalize. As stated previously, areas of relatively deep water with homogeneous characteristics would most likely not need this type of analysis, or even survey type as the MBES swath bathymetry increases in coverage area and can provide both bathymetry and BS without the need for SSS to cover any gaps.

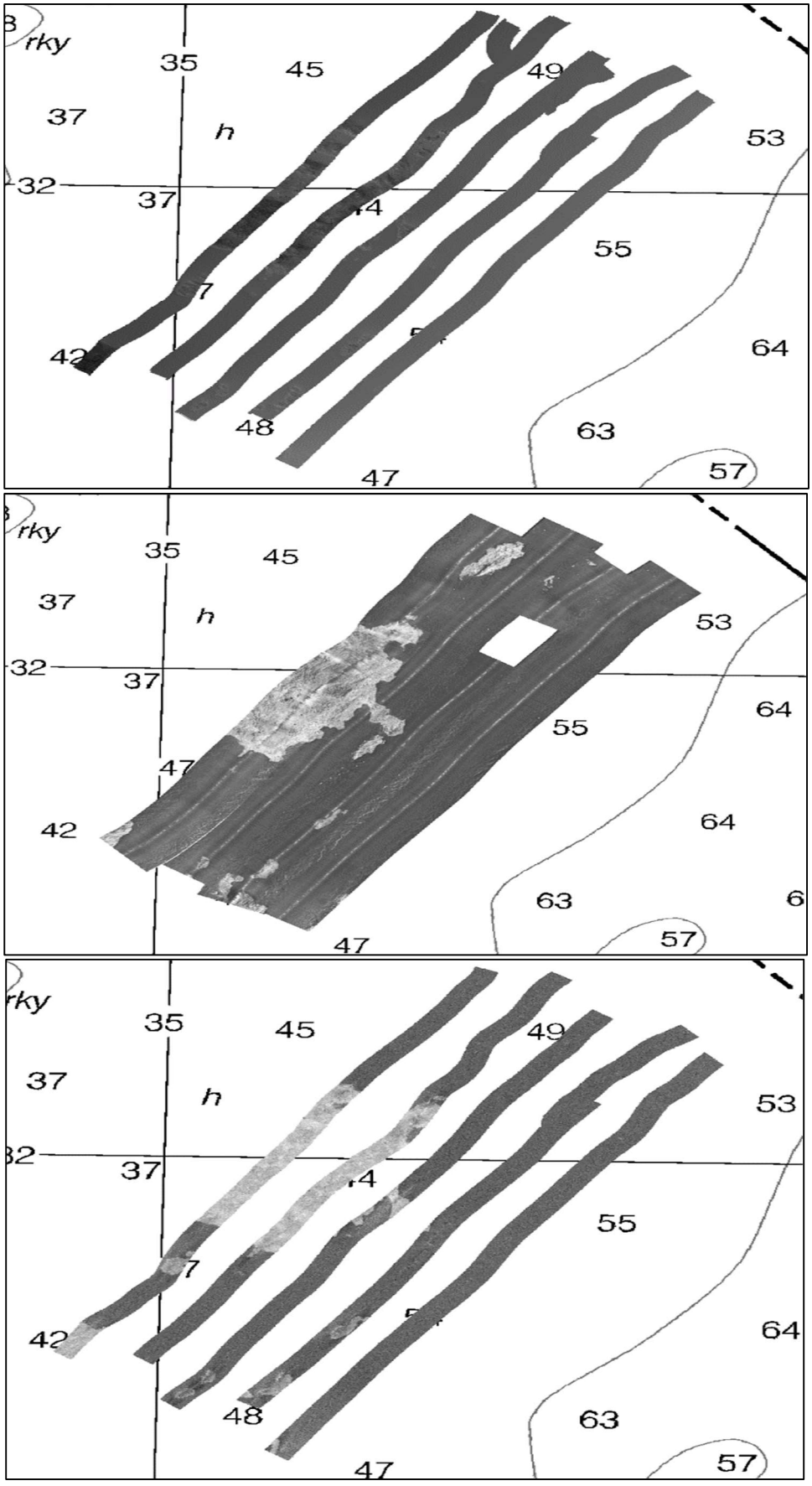

Figure 44: NW acquisition site: MBES (top), SSS (middle), and MBES Backscatter (bottom) prior to being overlaid.

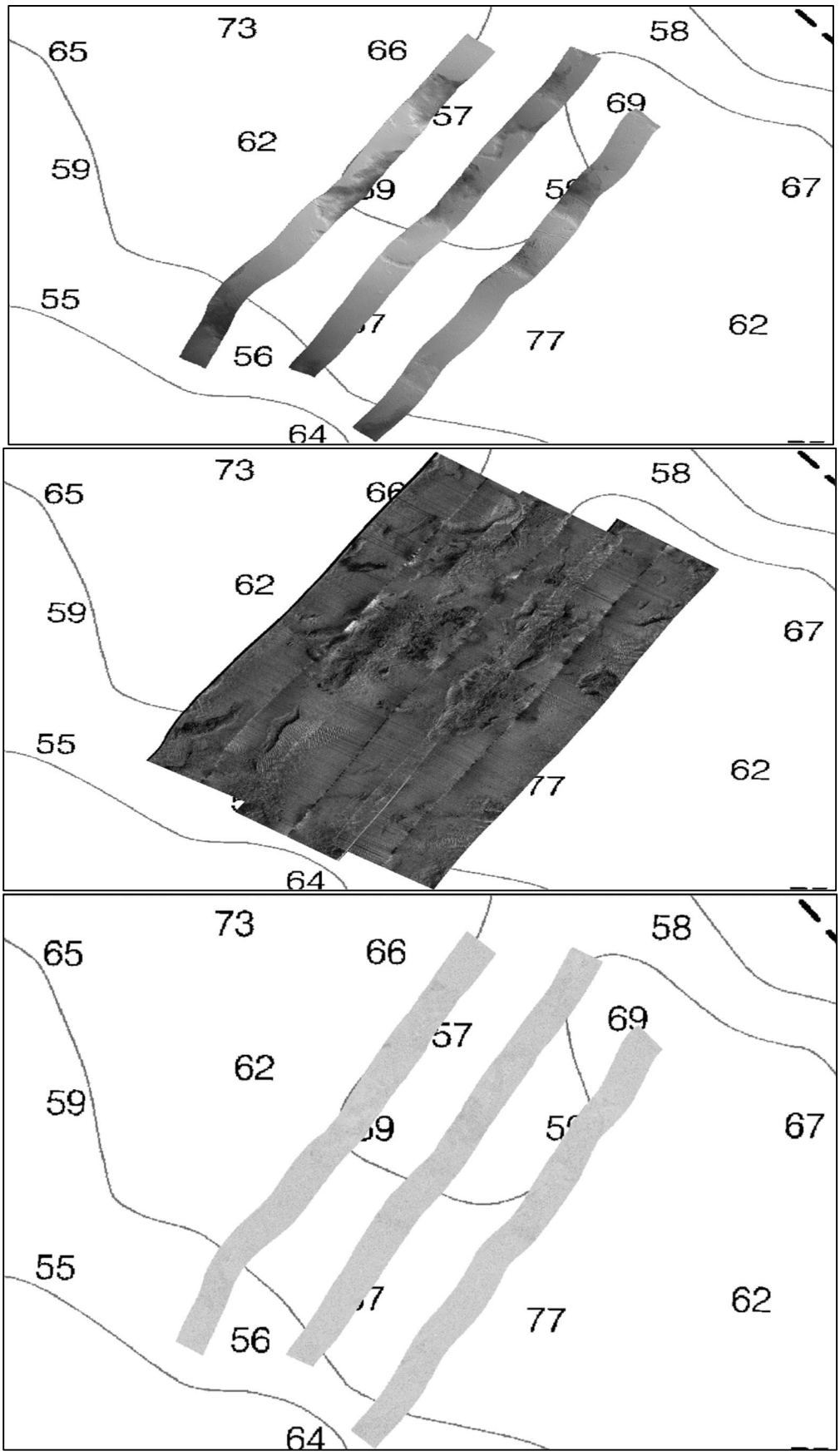

Figure 45: SE acquisition site: MBES (top), SSS (middle), and MBES Backscatter (bottom) prior to being overlaid.

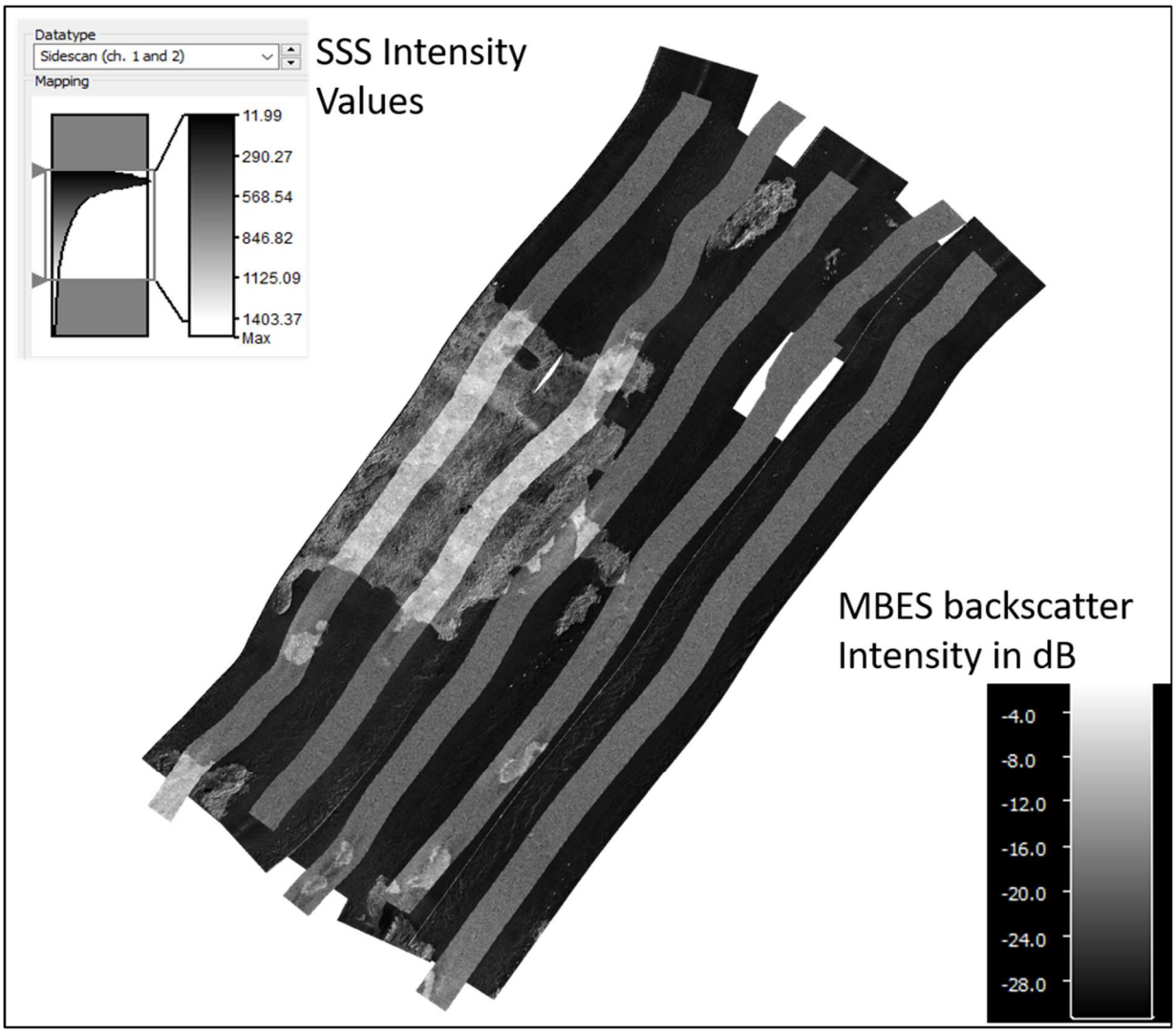

Figure 46: Initial comparison of the NW MBES backscatter in dB with the SSS imagery.

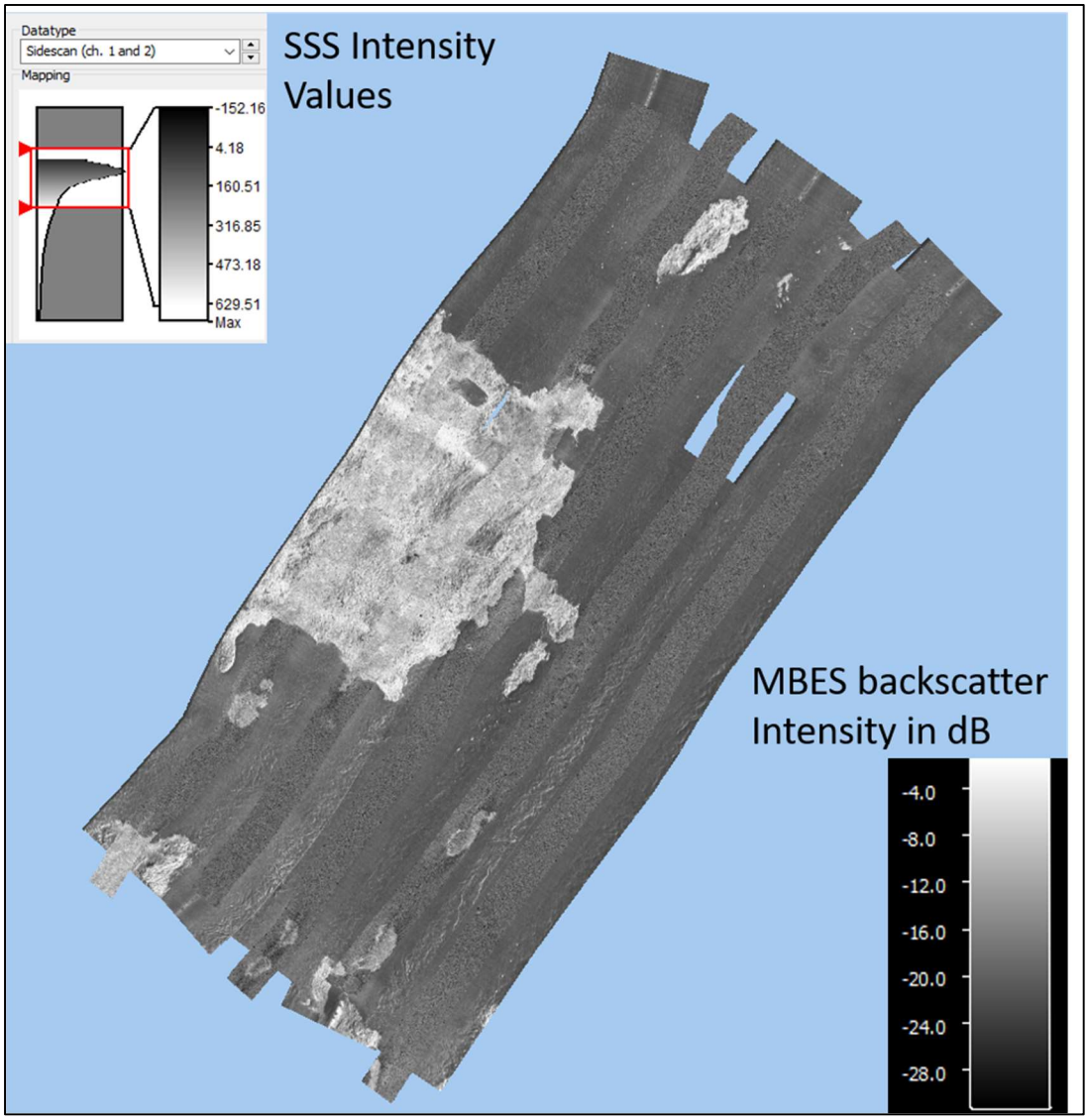

Figure 47: NW SSS and MBAB data after being adjusted to match intensity visualization.

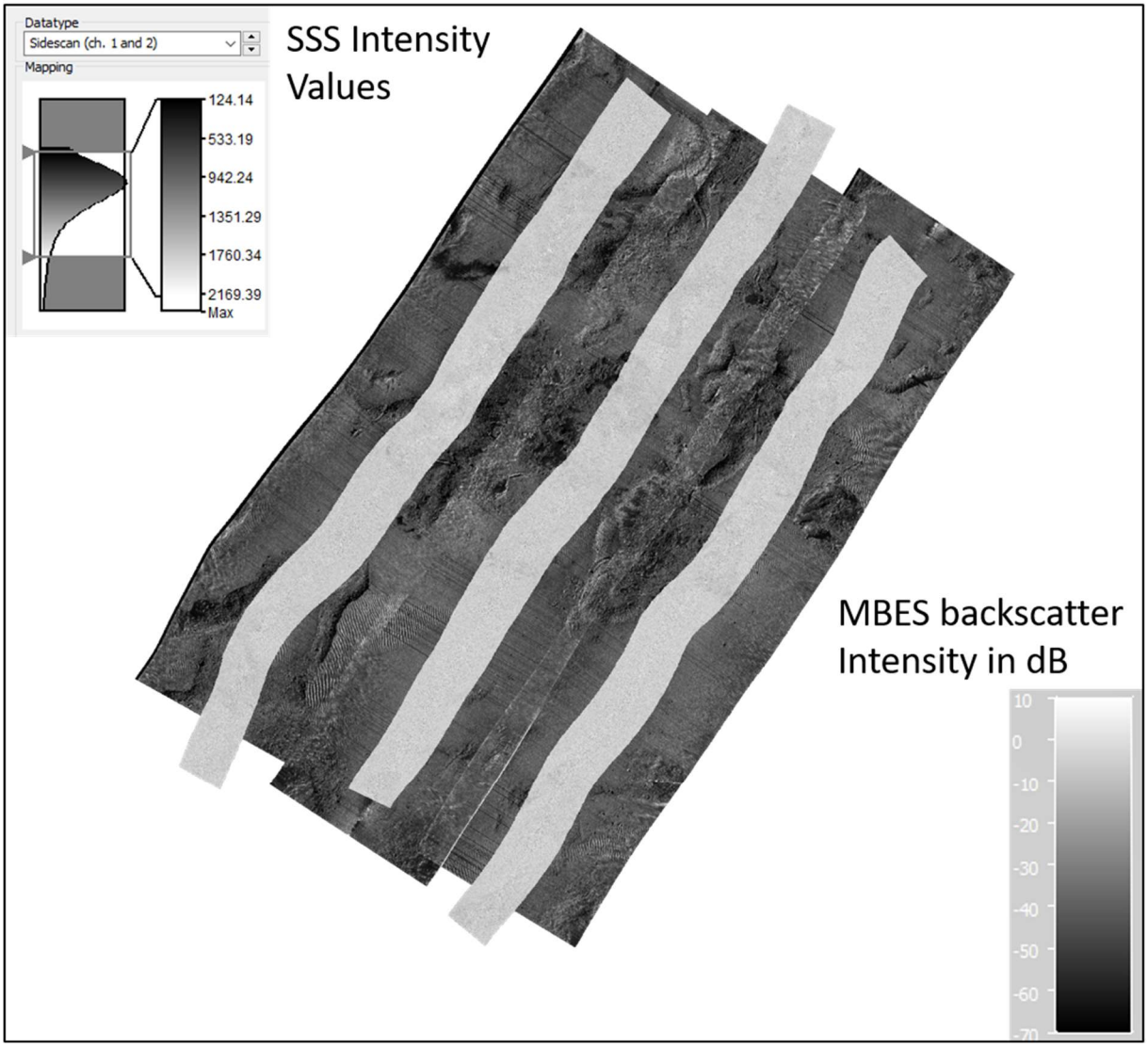

Figure 48: Initial comparison of the SE MBES backscatter in dB with the SSS imagery.

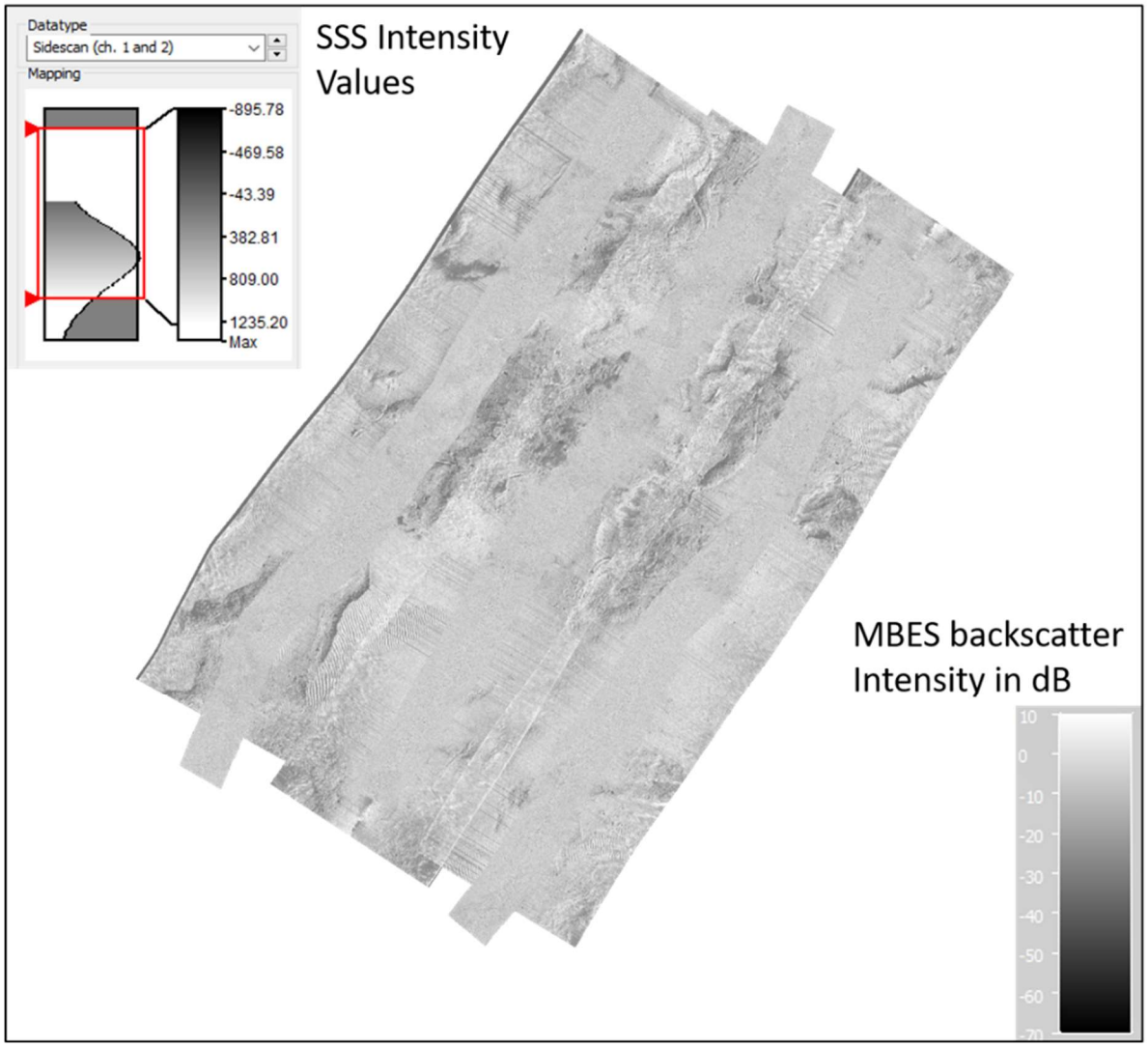

Figure 49: SE SSS and MBAB data after being adjusted to match intensity visualization.

Discussion

As the need for a more robust data set of seabed characterization arises, the ability to match data sets from different sensors provides a useful tool that is outside the scope of the typical NOAA OCS hydrographic survey paradigm. Through analysis of position and intensity disparities, one can create a mosaic that is not only precisely positioned, but has been adjusted so that both data types match in their respective backscatter intensities.

While this data set is relatively small, the boundaries of high BS intensity and low BS intensity in the NW survey site provide an effective measure for initial analysis. The SE survey site, while not precisely matching in either position or intensity, also provides valuable information for areas where

there may not be enough features to reference for position disparity and that is homogeneous in seabed characteristics and thus insufficient available dynamic range of backscatter observations to match. Both survey sites show that this process, as currently implemented, works best with seabed areas that exhibit both high and low contrast in their respective backscatter strength.

While proving to be a useful tool, the research conducted did show some limitations. Notably, the SSS imagery data used herein was represented in intensity values that were not represented in the same units as those of the MBAB. While a shortcoming for this research, the processes could be conducted, in part, in other software packages that produce SSS and MBES backscatter mosaics in the same intensity units. Related to the intensity values, another limitation is apparent. The intensity product that results from this research is still subjective and qualitative at this point. While the positioning disparity corrections are quantitative, the matching of the backscatter intensity, as implemented in this study, is solely at a visual level, and depends greatly on the user's interpretation of the corresponding backscatter intensities. It is possible for different users, looking at the same data set, to arrive at outcomes that do not match. Through repeated testing, I believe a standard procedure for adjusting intensities and creating standard mosaics is possible and could be developed in follow-on work. Alternately, and ideally, in the future there would be more communication between sonar manufacturers and software developers to ensure that the supplied backscatter units are understood and properly compensated for radiometric and geometric effects.

Another limitation that was found to be apparent, relates not only to the workflow, but also to the product of this research. This project showed how traditional surveys in shallow water areas of low relief, and homogeneous character, might not have noticeable finite features that exist in both the SSS and MBES bathymetry that can be used for the correction of position disparities. While areas such as some parts of the Arctic and some areas of the Gulf of Mexico are relatively featureless, one can find other ways to solve this problem. While finite features such as rocks may not be present, other identifiable features or seabed characteristics such as ice scours, anchor drags, and sand waves could be

used as reference points. An alternate and more ideal solution would be to investigate improved means of towfish positioning, such as USBL and integrated INS, which are now becoming standard in the commercial survey industry.

Despite the limitations, this tool proves to be in conjuncture with the philosophy within OCS of "ping once, use many times" and it is worthwhile to NOAA to invest the time and resources to create this product.

Acknowledgements:

I would like to thank my advisors Capt. Andy Armstrong (NOAA, Retired), and Dr. John Hughes Clarke for their expertise and patience in working with me on this project. I would also like to thank the professors and my fellow colleagues at the Center for Coastal and Ocean Mapping/Joint Hydrographic Center for their valuable instruction and help throughout this process.

I would further like to thank Dr. Peter Ramsay of Mind Technology-Klein for the use of the 4K-SVY Sidescan Sonar and Patrick Zynda from Chesapeake Technology for his amazing support and help in figuring out the processes in SonarWiz. I would also like to thank Kongsberg for the use of the EM2040P MBES.

To my fellow graduate students at CCOM, particularly LT. Patrick Debroisse (NOAA), and LTjg. Airlie Pickett (NOAA), thank you for always being there with a "you can do this" and for helping me with editing.

I would especially like to thank Dr. Larry Mayer of CCOM/JHC and those at NOAA's Office of Coast Survey who made this entire project possible by showing faith in me and selecting me for this opportunity.

Lastly, my deepest appreciation goes out to my mom and the rest of my family for always believing in me, and to my dog, Bailey, who put up with moving to New Hampshire and always being at the ready with a welcome home after my long days at school.

References:

Blondel, P. (2009). *The Handbook of Sidescan Sonar*. Springer.

Capus, C. G., Banks, A. C., Coiras, E., Tena Ruiz, I., Smith, C. J., & Petillot, Y. R. (2008). Data correction for visualisation and classification of sidescan SONAR imagery. *IET Radar, Sonar & Navigation*, *2*(3), 155. https://doi.org/10.1049/iet-rsn:20070032

Degel, C., Fonfara, H., Welsch, H. J., Becker, F. J., Hewener, H., Fournelle, M., & Tretbar, S. H. (2014). 3D sonar system based on mills cross antenna configuration. *2014 Oceans - St. John's*, 1–6. https://doi.org/10.1109/OCEANS.2014.7003133

Diaz, J. V. M. (1999). *Analysis of Multibeam Sonar Data for the Characterization of Seafloor Habitats* [Master of Engineering, University of New Brunswick]. https://hidrografica.tripod.com/Analysis_MB_SeafloorHabitats.pdf

EM 2040P MKII Multibeam echosounder, Max. 550 m. (n.d.). Retrieved November 5, 2021, from https://www.kongsberg.com/maritime/products/ocean-science/mapping-systems/multibeam-echo-sounders/em-2040p-mkii-multibeam-echosounder-max.-550-m/

Fakiris, E., Blondel, P., Papatheodorou, G., Christodoulou, D., Dimas, X., Georgiou, N., Kordella, S., Dimitriadis, C., Rzhanov, Y., Geraga, M., & Ferentinos, G. (2019). Multi-frequency, multi-sonar mapping of shallow habitats—Efficacy and management implications in the national marine park of zakynthos, greece. *Remote Sensing*, *11*(4), 461. https://doi.org/10.3390/rs11040461

Hammerstad, E. (2000). *EM technical note: Backscattering and seabed image reflectivity*. https://www.kongsberg.com/globalassets/maritime/km-products/product-documents/em_technical_note_web_backscatteringseabedimagereflectivity.pdf

Hellequin, L., Boucher, J.-M., & Lurton, X. (2003). Processing of high-frequency multibeam echo sounder data for seafloor characterization. *IEEE Journal of Oceanic Engineering*, *28*(1), 78–89. https://doi.org/10.1109/JOE.2002.808205

Hughes Clarke, J. (2004, May). *Seafloor Characterization using keel-mounted sidescan: Proper compensation for radiometric and geometric distortion*. Canadian Hydrographic Conference.

Hughes Clarke, J. (2012). Optimal Use of Multibeam Technology in the Study of Shelf Morphodynamics. In *Sediments, Morphology and Sedimentary Processes on Continental Shelves* (pp. 1–28). John Wiley & Sons, Ltd. https://doi.org/10.1002/9781118311172.ch1

Hughes Clarke, J. E. (2020, December 5). *C20: Multibeam Backscatter Imaging*.

Lamarche, G., & Lurton, X. (2018). Recommendations for improved and coherent acquisition and processing of backscatter data from seafloor-mapping sonars. *Marine Geophysical Research*, *39*(1–2), 5–22. https://doi.org/10.1007/s11001-017-9315-6

Leblond, I., & Bertholom, A. (2020). Towed sensors positioning with forward looking sonars: Application on a Side Scan Sonar. *E-Forum Acusticum 2020*, 1981–1988. https://doi.org/10.48465/fa.2020.0315

Shang, Zhao, & Zhang. (2019). Obtaining high-resolution seabed topography and surface details by co-registration of side-scan sonar and multibeam echo sounder images. *Remote Sensing*, *11*(12), 1496. https://doi.org/10.3390/rs11121496

SIS Seafloor Information System Reference Manual Release 5.6. (2021). Kongsberg Maritime. https://www.kongsberg.com/contentassets/cdfaccc0be8040108b46bae537b26d13/429004e_sis5_ref.pdf

SonarWiz 7.08 User Guide. (2021). Chesapeake Technology, Inc. www.chesapeaketech.com

Sternlicht, D. D. (2017). Historical development of side scan sonar. *The Journal of the Acoustical Society of America*, *141*(5), 4041–4041. https://doi.org/10.1121/1.4989335

Vilming, S. (1998). The development of the multibeam echosounder: An historical account. *The Journal of the Acoustical Society of America*, *103*(5), 2935–2935. https://doi.org/10.1121/1.422177